


RESEARCH ARTICLE



Small intestine is not colon: a new *in vitro* model of the human ileum microbiome integrating the mucosal microenvironment and feeding status

Auriane Bron^{a,b,c,d,1}, Chloé Beltramo^{a,b,c,d,1}, Claude Durif^{a,c,d}, Trisha Arora^{e,f,g}, Charlotte Deschamps^{a,c,d}, Ingrid Couturier^{a,c,d}, Xavier Domingo-Almenara^{e,f,g}, Yolanda F. Otero^h, Sylvain Denis^{a,c,d}, Tom Van de Wiele^{b,c,d}  and Stéphanie Blanquet-Diot^{a,c,d}

^aUMR 454 MEDIS UCA-INRAE, Microbiology, Digestive Environment and Health, Université Clermont Auvergne, Clermont-Ferrand, France; ^bCenter for Microbial Ecology and Technology (CMET), Department of Biotechnology, Ghent University, Ghent, Belgium; ^cInternational Associated Laboratory Host Microbes Interactions in the Human Gut (HOMIGUT), Ferrand, France; ^dInternational Associated Laboratory Host Microbes Interactions in the Human Gut (HOMIGUT), Ghent, Belgium; ^eEurecat, Technology Center of Catalonia, Reus, Spain; ^fDepartment of Electrical, Electronic and Control Engineering (DEEEA), Universitat Rovira i Virgili, Tarragona, Spain; ^gCentre for Omics Sciences (COS), Eurecat - Technology Centre of Catalonia, Rovira i Virgili University Joint Unit, Uniqe Scientific and Technical Infrastructures (ICTS), Reus, Spain; ^hValbion Research & Development Riom Center, Riom, France

ABSTRACT

The small intestinal microbiota plays a key role in human health but is understudied due to the invasiveness of sampling. There is no available model of the human ileal microbiome simulating the key nutritional and physicochemical parameters shaping this ecosystem, which has been fully validated based on *in vivo* data. Here, the Mucosal Artificial Ileum (M-ARILE) was set up to reproduce the pH, transit time, anoxic conditions, dynamics of feeding and microenvironments (luminal *versus* mucosal) found in a healthy human mid-ileum. To validate the newly developed *in vitro* system, nine-day fermentations were performed under either ileal or colonic conditions using the same fecal inoculum ($n = 3$ adult volunteers). The gut microbiota composition and metabolic activities were monitored daily. Distinct microbial signatures and metabolite profiles were obtained between *in vitro* ileum and colon conditions. In accordance with *in vivo* data, *Peptostreptococcaceae*, *Clostridiaceae* and *Enterococcaceae* were enriched in the ileum and associated with lower short-chain fatty acid production but higher O_2 percentages. Interestingly, the abundances of key populations, such as *Akkermansiaceae*, and bile acid profiles were dependent on the feeding status of the M-ARILE. This new model provides a powerful platform for mechanistic studies on the role of ileal microbes in human nutrition and health considering inter-individual variabilities.

ARTICLE HISTORY

Received 24 March 2025
Revised 29 September 2025
Accepted 20 October 2025

KEYWORDS


in vitro gut model;
microbiota; small intestine;
colon; M-ARILE; mucus; fed/
fasted states; SCFA; bile
acids; metabolomics.

Introduction

The small intestine is the primary site of food digestion and nutrient absorption in humans, playing a key role in maintaining health.¹ It consists of three anatomically distinct compartments: a short segment, the duodenum, followed by two longer ones, the jejunum and the ileum.² Digestive enzymes produced by the pancreas, along with bile from the liver, are secreted into the duodenum, where they facilitate the breakdown and intestinal absorption of carbohydrates, proteins and lipids, while undigested compounds are delivered to the large intestinal compartment.^{2,3} The small intestine is characterized by a high level of dynamics in several key physicochemical factors, such as the feeding status, alternating between fed *versus* fasted periods,⁴ nutrient availability and the oxygen level, which decrease from the proximal to the distal sections, while the pH and transit time increase. Shifts in the nutritional and physicochemical conditions along the small intestine are shaping its microbial composition and abundance. The digestive lumen is colonized by a diverse microbiota, mainly belonging to the

CONTACT Stéphanie Blanquet-Diot  stephanie.blanquet@uca.fr  Université Clermont Auvergne, UMR 454 MEDIS UCA-INRAE, Microbiology, Digestive Environment and Health, 28 place Henri Dunant, F-63000, Clermont-Ferrand, France

¹These authors contributed equally.

 Supplemental data for this article can be accessed online at <https://doi.org/10.1080/19490976.2025.2579353>.

© 2025 The Author(s). Published with license by Taylor & Francis Group, LLC.

This is an Open Access article distributed under the terms of the Creative Commons Attribution-NonCommercial License (<http://creativecommons.org/licenses/by-nc/4.0/>), which permits unrestricted non-commercial use, distribution, and reproduction in any medium, provided the original work is properly cited. The terms on which this article has been published allow the posting of the Accepted Manuscript in a repository by the author(s) or with their consent.

bacterial phyla *Bacillota*, *Pseudomonadota*, *Bacteroidota*, *Fusobacteriota* and *Actinomycetota*.¹ Scarce studies have shown that the mucosal microbial composition differs from that of the lumen due to the mucus layer acting both as a physical barrier and a reservoir for microbial colonization.⁵ Bacterial loads increase from 10^3 CFU/mL in the duodenum to 10^7 – 10^8 CFU/mL in the ileum, with a corresponding rise in bacterial diversity and proportion of anaerobic bacteria.⁶ These changes are amplified in the human colon, which has the highest bacterial load (10^{11} – 10^{12} CFU/mL), diversity and number of anaerobes in the digestive tract. The fermentation of undigested dietary components by gut bacteria in the small intestine mainly produces short-chain fatty acids (SCFAs), though in ten times lower amounts compared to the large intestine, due to less active fermentation activity.⁷

Alterations in the small intestinal microbiota have been linked to various human diseases, such as small intestinal overgrowth (SIBO), characterized by excessive bacterial numbers, leading to bloating, diarrhea and abdominal discomfort as symptoms.⁸ However, studying the role of small intestinal microbes in human nutrition-health and disease is challenging due to the difficulty and invasiveness of sampling methods, such as duodenojejunal aspiration, ileostomy, and surgery, often leading to only postmortem collection.^{9,10} Most research in humans, to date, has focused on fecal and, to a lesser extent, colonic microbes, which widely differ in composition, diversity and function from small intestinal microorganisms.¹¹ An alternative approach is the use of *in vitro* models simulating the human small intestine and its microbial component. Currently, no *in vitro* model fully replicates the microbial ecosystem of the human duodenum or jejunum, and only a few studies have reported the development of *in vitro* models of the human ileal microbiota. One such model, which is based on the TNO gastrointestinal system (TIM), was inoculated with ileostomy effluent or fecal material to integrate ileal microbes.¹² Another model, known as The Smallest Intestine (TSI), incorporates a consortium of seven representative bacterial species from the ileum in a monocompartmental system.¹³ Additionally, the multicompartmental Simulator of the Human Intestinal Microbial Ecosystem (SHIME) and its mucosal configuration (M-SHIME) have been used to reproduce the ileal microbiota through a minute retrograde inoculation from the proximal colon into the ileum compartment¹⁴ or the addition of a consortium of twelve bacteria.¹⁵ However, none of those models combines the complexity and dynamism of the ileal environment (such as the differentiation between luminal and mucosal compartments and nutrient availability associated with fed and fasted states), along with in-depth validation against humans *in vivo* data.

In this context, the main objective of our study was to set up a new model of the healthy human mid-ileal compartment based on *in vivo* data, accurately reproducing the key physicochemical, nutritional and microbial characteristics of this environment. This model, named Mucosal Artificial Ileum (M-ARILE), was derived from the previously well-described Mucosal Artificial Colon (M-ARCOL).^{16,17} To validate the new M-ARILE configuration, a fecal sample from a healthy adult volunteer ($n = 3$) was used to inoculate two bioreactors running in parallel for 10 d, each simulating either ileal or colonic human conditions. The ileal microbiota composition and function were monitored over time and compared to both colonic results and *in vivo* data in humans from the literature.

Materials and methods

Fecal sample collection and treatment

Stool samples used to inoculate bioreactors were collected from three healthy adult volunteers (mean age: 41.7 ± 15 y): two men aged 43 and 56 y (donors M1 and M2, respectively) and one woman aged 26 y (donor F1). All the donors had no history of antibiotic treatment or probiotic-prebiotic consumption three months prior to stool collection. All the donors provided written and informed consent to participate in the study. The use of fecal microbiota from human origin was approved by the ethical committee under registration number MEDIS MICROVITRO 2022-A02066–37. Feces were collected in a sterile recipient, placed in an airtight anaerobic box (GENbag anaer gas pack systems, Biomerieux, France), transported at ambient temperature to the laboratory and processed within 6 h following defecation. In an anaerobic chamber (Pure evo T4, Jacomex, France), each fecal sample was manually homogenized, and 10 g of feces were resuspended in 30 mM sterile sodium phosphate buffer (pH 6.6) to reach a total volume of 200 mL. The fecal suspension was then mixed and filtered (500 µm inox

sieve) before M-ARCOL inoculation (10^9 CFU/mL). For M-ARILE, serial dilutions were made in 30 mM sterile sodium phosphate buffer (pH 7.2, 100 mL) to reach an initial bacterial load of 10^7 CFU/mL.

Description and set-up of the *in vitro* models

The *in vitro* models of the ileal (M-ARILE) and colonic (M-ARCOL) compartments were composed of a main bioreactor (MiniBio, Applikon, Delft, The Netherlands) connected to an external glass compartment containing mucin-alginate beads, which reproduce the luminal and mucosal microenvironments, respectively (Figure 1). The bioreactors were kept at body temperature using heating blocks. The pH and redox

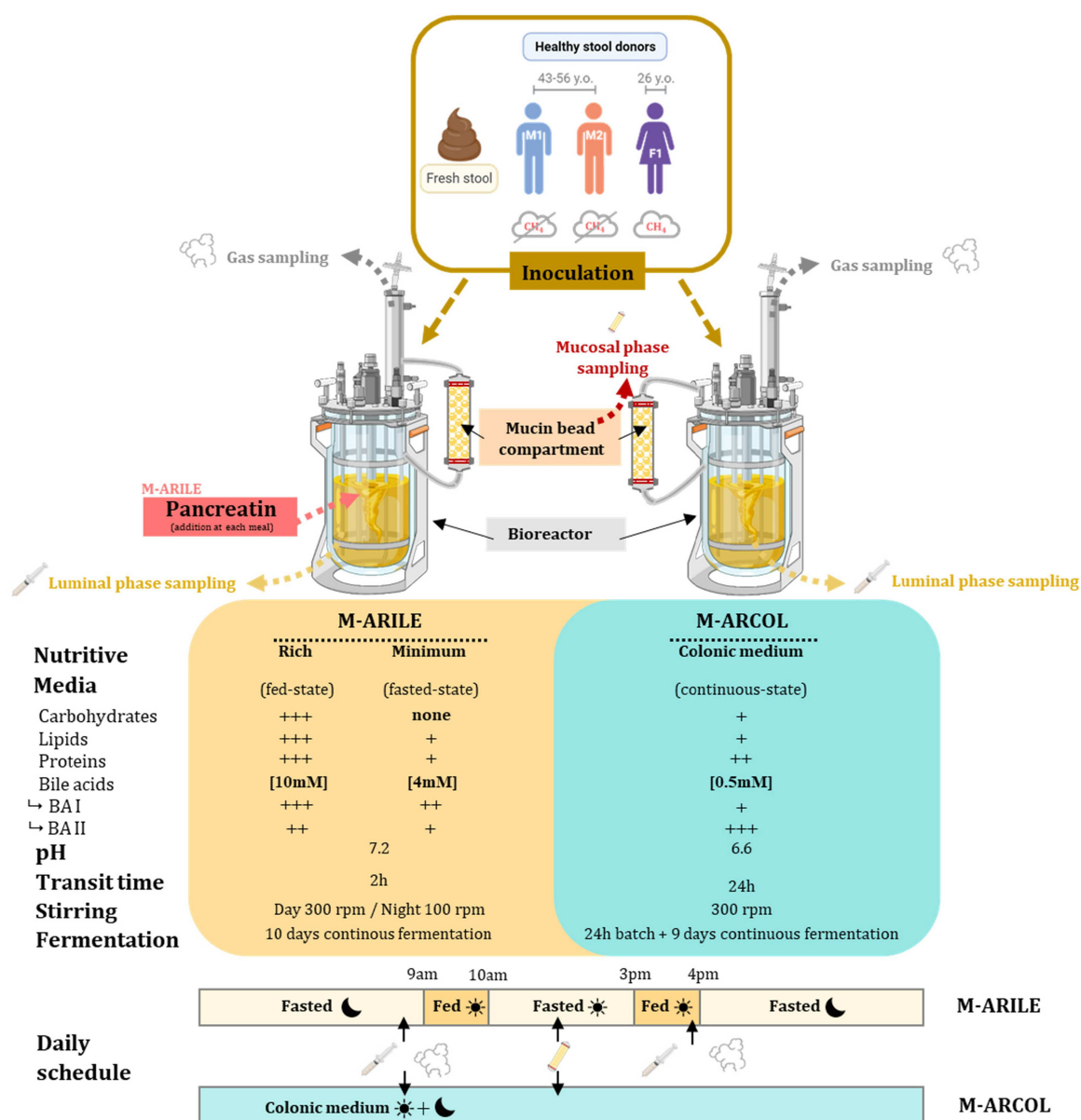


Figure 1. Experimental set-up, sampling procedure and analysis performed during M-ARILE and M-ARCOL *in vitro* fermentations. Once set-up with physicochemical and nutritional parameters specific from human ileal (M-ARILE) or colonic (M-ARCOL) compartments, the two models were inoculated with a fecal sample from one healthy adult and run in parallel for 10 d, including 1 day of batch microbiota amplification for M-ARCOL. The fed and fasted states were reproduced in the M-ARILE. The experiments were replicated using stools from three donors (two males and one female). Samples were regularly collected from the main bioreactor (luminal compartment), mucin beads (mucosal compartment) and the atmospheric phase for further analysis of microbiota composition (quantitative PCR and 16S metabarcoding) and metabolic activities (short-chain fatty acid and gas).

potential were constantly recorded (Applikon, Delft, The Netherlands), and the pH was adjusted to the set-points with 1 M NaHCO₃. At the beginning of the experiment, the fecal suspensions were introduced into the main bioreactors diluted in the appropriate nutritive media, i.e., mid-ileal medium under fasted condition for M-ARILE and colonic medium for M-ARCOL (Table 1). Ileal or colonic nutritive media were introduced into the main bioreactors, while fermentation media were automatically withdrawn, ensuring the appropriate mean ileal or colonic retention times. After an initial sparging of O₂-free N₂ gas, anaerobiosis was maintained during the total course of fermentation by the sole activity of the resident microbiota and through ensuring system airtightness. The mucosal compartment was submerged in a water bath maintained at body temperature and filled with mucin-alginate beads, offering an overall surface area of 723 cm² on average. To produce mucin beads, mucin type II from porcine stomach (Sigma-Aldrich, Saint-Louis, MO, USA) and sodium alginate (Sigma-Aldrich, Saint-Louis, MO, USA) were diluted in sterile distilled water at concentrations of 5% and 2%, respectively, and the pH was adjusted to approximately 7 with a sodium bicarbonate solution (1 M). A peristaltic pump was used to drop the mucin-alginate solution into a sterile solution of 0.2 M CaCl₂ dihydrate under agitation. Every two days, mucin-alginate beads remaining in the mucosal compartment were collected and renewed with fresh sterile ones, while anaerobiosis was assured by a CO₂ flush prior reconnection to the fermentation system. In the present study, all the parameters were adjusted to reproduce the mean conditions found in the ileum or large intestine of healthy adults, as described in Table 1.

Experimental design and sampling

For each fermentation run (Figure 1), two bioreactors inoculated with a fecal sample from a unique healthy adult donor were run in parallel, one reproducing the ileal condition (M-ARILE configuration), while the other simulated the colonic one (M-ARCOL). Fermentations were run under batch condition for 24 h and then under continuous conditions for nine additional days in the M-ARCOL, and directly under continuous conditions for ten days in the M-ARILE. Experiments were performed in triplicate using fecal inoculum from three different donors. Samples were collected twice a day in the main bioreactors (corresponding to the luminal phase) for further analysis of microbiota composition (qPCR and 16S rDNA metabarcoding) and metabolic activities through targeted approaches (SCFA and bile acid measurements) and nontargeted metabolomics. The atmospheric phase was also sampled twice a day to follow anaerobiosis, and the gas composition and production using a sampling bag connected to the system. Every two days, mucin beads were collected and washed twice in sterile phosphate-buffered saline (PBS) prior to mucus-associated microbiota analysis. All samples were stored at −80 °C before downstream analysis.

Table 1. Physicochemical and nutritional parameters used to set-up the M-ARILE (ileal, under both fasted and fed states) and M-ARCOL (colon) models.

Parameters		M-ARILE fasted	M-ARILE fed	M-ARCOL
Medium	Carbohydrates (g/L)	0	21.3	7.0
	Fibers (g/L)	0	14.1	7.5
	Proteins (g/L)	2.1	34.8	12.0
	Lipids (g/L)	0.6	20.6	1.5
	Mucin (g/L)	1.5	1.5	4.0
	Vitamin/oligoelements (µg/L)	464.7	464.7	464.7
	Electrolytes (g/L)	8.5	8.5	11.1
	Bile acids	Total (mM)	4	0.5
		Primary	++	+
		Secondary	+	+++
Stirring (rpm)	Day	300		300
	Night	100		
pH		7.2		6.6
Inoculation rate (CFU/mL)		10 ⁷		10 ⁹
Transit time (h)		2		24
Mucin beads (cm ²)			723	

CFU: colony forming unit; M-ARILE: Mucosal Artificial Ileum; M-ARCOL: Mucosal Artificial Colon; + to +++: low to high concentrations.

DNA extraction and quality control

The QIAamp Fast DNA Stool Mini Kit (Qiagen, Hilden, Germany) was used to extract genomic DNA from luminal samples, following the manufacturer's instructions with the following adaptations.¹⁶ Prior to DNA extraction, one milliliter of luminal sample was centrifuged ($18,000 \times g$, 15 min, 4 °C), and pellets were collected. A step of mechanical disruption using a bead beater (5 min, 20 beats/sec) was performed with 300 mg sterile glass beads (diameter ranging from 100 to 600 μ m) before extraction with the kit. A Quick DNA Fecal/Soil Microbe Miniprep Kit (Zymo Research, Orange, California) was used for DNA extraction from mucin-alginate beads. The manufacturer's instructions were followed with 150–200 mg of mucin-alginate beads. The quality of the DNA extracts was evaluated via a NanoDrop 2000 (Thermo Fisher Scientific, Waltham, Massachusetts, USA). DNA quantity was measured using the Qubit dsDNA Broad Range Assay Kit (Invitrogen, Carlsbad, CA, USA) with a Qubit 3.0 fluorometer (Invitrogen, Carlsbad, CA, USA). The DNA was stored at –20 °C prior to further analysis.

Quantitative PCR

Total bacteria, *Bacteroidetes*, *Firmicutes* and *γ -Proteobacteria* were quantified via qPCR using primers and conditions described in Table 2. A Biorad CFX96™ Real-Time System (Bio-Rad Laboratories, Hercules, CA, USA) with a Takyon™ Low ROX SYBR® 2X MasterMix blue dTTP kit (Eurogentec, Seraing, Belgium) was used to perform the qPCR assays. Each reaction was run in duplicate in a final volume of 10 μ L with 5 μ L of MasterMix, 0.45 μ L of each primer (10 μ M), 1 μ L of DNA sample and 3.1 μ L of ultrapure water. The protocol used for amplification was as follows: 1 cycle at 95 °C for 5 min, followed by 40 cycles of 95 °C for 30 s and then 58 °C for 30 s. A melting step was added to ensure primer specificity. Standard curves were generated from 10-fold dilutions of bacterial DNA (extracted from a fermentation sample), allowing the calculation of DNA concentrations as previously described.¹⁸

16S rDNA metabarcoding and data analysis

Bacterial V3-V4 regions of 16S ribosomal DNA (rDNA) and the archaeal 16S rDNA were amplified using primers described in Table 2. Amplicons were generated using a Fluidigm Access Array followed by high-throughput sequencing on an Illumina MiSeq system (Illumina, IL, USA) performed at the Carver Biotechnology Center of the University of Illinois (Urbana, USA). Bioinformatic analysis was performed using R studio software (version 4.2) and the rANOMALY package.²³ Prior to analysis, the raw data were demultiplexed and quality filtered using DADA2 R package.²⁴ Reads with *N* bases or low Phred quality scores (less than or equal to 2) were eliminated, and reads under 100 bp in length were removed. Decontamination steps were carried out to filter out sequences corresponding to PhiX DNA used as a spike-in control for MiSeq runs. Filtered sequences were dereplicated and cleaned for chimeras (DADA2), and amplicon variant sequences (ASVs) were inferred using the dada function of the DADA2 R package.

Table 2. Primers used for qPCR and 16S rDNA Metabarcoding analysis.

Primer names	Sequence 5'-3'	Target	Annealing temperature (°C)	References
qPCR primers				
BAC516F	GTATTACCGGGCTGCTG	Total bacteria	58	[19]
BAC338R	ACTCTACGGGAGGCAG			
789cfbF	CRAACAGGATTAGATACCT	<i>Bacteroidetes</i>	61	[20]
cfb976R	GGTAAGGTTCTCGCGTAT			
928F-Firm	TGAAACTYAAAGGAATTGACG	<i>Firmicutes</i>	61	[20]
1040FirmR	ACCATGCACCACTGTC			
1080yF	TCGTCAGCTCGTGTGTGA	<i>γ-Proteobacteria</i>	56	[20]
y1202R	CGTAAGGGCCATGATG			
Metabarcoding primers				
V3_F357_N	CCTACGGGNGGCWGCAG	<i>Bacteria</i>	–	[21]
V4_R805	GACTACHVGGGTATCTAATCC			
Arch349F	GYGCASCAGKCGMGAAW	<i>Archaea</i>	–	[22]
Arch806R	GGACTACVSGGGTATCTAAT			

qPCR: quantitative polymerase chain reaction.

Taxonomic affiliation was performed with *idtaxa* function from the DECIPHER package²⁵ using the SILVA release 138 database.²⁶ A phylogenetic tree was constructed based on ASVs representative sequences using functions from the *phangorn* package.²⁷

Gas analysis

The amounts of O₂, N₂, CO₂, CH₄ and H₂ gases found in the atmospheric phases of bioreactors were analyzed with a 490 microgas chromatographs (Agilent Technologies, Santa Clara, CA, USA) coupled with a micro-TCD detector (Agilent Technologies, Santa Clara, CA, USA). Molecular sieve 5 A and Porapak Q (Agilent Technologies, Santa Clara, CA, USA) series columns were used. Ambient air and three gas mixtures were used to construct calibration curves (ambient air: 78.09% N₂, 20.95% O₂, 0.04% CO₂; mixtures A: 5% CO₂, 5% H₂, 90% N₂; B: 20% CO₂, 80% H₂; C: 20% CO₂, 20% CH₄, 20% H₂, 40% N₂). The results are expressed as relative percentages. The total gas volume was also measured daily using a syringe.

Short-chain fatty acid analysis

Luminal samples (1.5 mL) were centrifuged (18,000 × g, 15 min, 4 °C), and 900 µL of the supernatant were diluted to 1.22 in H₂SO₄ 0.04 M mobile phase, vortexed and filtered (0.22 µm pore size). The three major SCFAs (i.e., acetate, propionate, and butyrate) were quantified via high-performance liquid chromatography (HPLC, Elite LaChrom, Merck HITACHI, USA) coupled with a DAD detector (λ = 205 nm). Elution was performed with an ICE-COREGEL 87H3 9 µm 150 × 7.8 mm column and a guard column (Concise Separations, San Jose, CA, USA) maintained at 50 °C with 0.04 M sulfuric acid as the mobile phase (0.6 mL/min). The data were analyzed via EZChrom Elite software. SCFA concentrations were calculated from standard curves established with known equimolar concentrations of acetate, propionate, and butyrate (0, 10, 25 and 40 mM), and the results are expressed as mM or relative percentages.

Metabolomic analysis

Luminal samples collected from M-ARILE and M-ARCOL at days 7, 8 and 9 were analyzed via targeted and nontargeted metabolomics. Bile acids and SCFAs were quantified with liquid chromatography (LC) and gas chromatography (GC), coupled with tandem mass spectrometry (LC-MS/MS and GC-MS/MS, respectively), and optimized multiple reaction monitoring (MRM) transitions were used. Targeted metabolomics data were processed with Agilent MassHunter Quantitative Analysis (version 10.1). Absolute quantification was performed with a calibration curve prepared with an analytical standard for each bile acid and SCFA. Polar metabolite profiling was performed using GC coupled with a quadrupole time-of-flight (qTOF) mass spectrometer configured in full-scan mode. Vendor-specific raw data were converted to mzXML files format using Proteowizard. The R package eRah version 2.0.1^{28,29} was used for deconvolution, alignment, quantification and metabolite identification. The experimental deconvolved spectra were matched to metabolite reference spectra and retention index (RI) data using the Golm Metabolome Database. Finally, 54 metabolites were manually annotated with RI error <1% and spectral similarity >80%. Additional details on metabolite extraction, acquisition methods and data analysis are included in the Supplementary Materials (Suppl. Methods, Suppl. Table 1 and Suppl. Table 2).

Statistical analysis

Statistical analyses of microbiota activity (gas and SCFAs) were processed using GraphPad Prism software (version 9). The normal distribution of the data was verified by combining the Anderson-Darling, D'Agostino, Pearson, Shapiro-Wilk, and Kolmogorov-Smirnov tests. Then, appropriate statistical analysis was applied (unpaired t tests or Wilcoxon-Mann-Whitney tests). A *P* value < of 0.05 was considered statistically significant. Metabarcoding analysis, including α-diversity indices (number of observed ASVs

and Shannon index) and statistical analysis of the metabolomic data, were processed using R software (version 4.2). Principal coordinate analysis (PCoA) was performed to highlight important donor effects. Constraint redundancy analysis (RDA) was then performed with time, microenvironment (luminal *versus* mucosal), feeding status (fasted *versus* fed) and experimental conditions (M-ARILE *versus* M-ARCOL) as variables of the model first with all parameters and then with removal of the donor effect. Bray Curtis distances were used for each analysis, and the significance between groups was assessed with one- or two-way ANOVA. Differential analyses (DESeq2, metagenomeSeq, metacoder) were performed using rANOMALY package.²³ The R package vegan (version 2.6–4) was used to perform the RDA analysis while ggpubr (version 0.6.0) was used for making the boxplots. Spearman correlation analyses were performed, and associated heatmaps were generated using the microeco package (version 1.6.0).³⁰ The metabolomic statistical analysis was performed with R (version 4.3.1) using the same packages as previously mentioned. RDA was run using Euclidean distance without a donor effect. Statistical significance was calculated using the Wilcoxon test unless otherwise specified.

Results

Adaptation of the *in vitro* colon model (M-ARCOL) to the specific human ileal digestive conditions (M-ARILE)

Our large literature survey on healthy human adult ileum¹ served as a valuable information source to adapt the nutritional and physicochemical parameters of the M-ARCOL, developed to reproduce human colonic conditions, to those of the mid-ileum, leading to the M-ARILE configuration. The body temperature was maintained at 37 °C, and the pH was increased to 7.2 according to the mean values found in the literature.^{31–33} The ileum transit time was reduced to 2 h based on *in vivo* measurements.^{34–36} The bacterial inoculation density was decreased from 10⁹ in the fecal solution to 10⁷ CFU/mL in the M-ARILE to reproduce the lower microbial load found in the ileal compartment compared to the colonic one.^{11,37} In addition, we adapted the composition of the nutritive media to better mimic the nutrients found in the human small intestine and simulate the alternance between fasted and fed states. A ‘rich medium’ was defined to reproduce a fed state in the M-ARILE, while a ‘minimum medium’ was used under the fasted state. Compared to the M-ARCOL nutritive medium, the concentrations of digestible carbohydrates, proteins and lipids were increased in the rich medium, as these nutrients are found at a higher level in the mid-ileum of healthy adult humans compared to the colon.¹ The amount of monosaccharide (glucose) and soluble fibers was also increased in the rich medium of M-ARILE compared to M-ARCOL,² while the minimum medium contained no digestible carbohydrate and, 16- and 37-fold less proteins and lipids respectively than the rich medium.³⁸ Bile salts concentrations were increased in the M-ARILE nutritive medium compared to M-ARCOL ones, to take into account that 95% of total bile acids are reabsorbed in the terminal ileum,³⁹ with higher amounts in the fed (10 mM) compared to the fasted (4 mM) nutritive medium.^{40,41} The ratio between primary and secondary bile salts was also increased in the M-ARILE considering their metabolism by gut microbes from ileal to colonic compartment.^{40,42} Vitamins, oligo-elements and electrolytes were unchanged between the two models.² Lastly, stirring was reduced during the night phase in the M-ARILE (100 rpm *versus* 300 rpm during the day) to mimic lower small intestinal peristaltic activities that occur during the night.⁴³ All the parameters used to set-up the new M-ARILE configuration are summarized in Table 1.

Microbiota metabolic activities under ileal versus colonic conditions

Ileal or colonic pH and redox potential were continuously monitored inside the bioreactors, as an indirect indicator of microbiota metabolic activities (Suppl. Figure 1 and Suppl. Figure 2). Ileal pH repeatedly decreased below 7.2 during all the feeding periods, indicating intermittent acidification associated with higher microbial fermentation activities, whereas the pH in M-ARCOL rapidly stabilized at the set-point value (6.6) (Suppl. Figure 1). Similarly, lower redox potential values were observed during fed periods in the M-ARILE before reincreasing to approximately –230 mV during fasted states, while it rapidly

stabilized around -250 mV in the M-ARCOL for all donors (Suppl. Figure 2). Gas and SCFA levels were monitored throughout fermentation to determine the length of the stabilization period in both *in vitro* models. Gas profiles stabilized for all donors at day 4 in the M-ARILE compared to day 2 in the M-ARCOL (Figure 2A). As expected, high percentages of O_2 remained in the ileum atmospheric phase, ranging from 2.3 to 6.4% depending on the donor. In contrast, anaerobiosis was efficiently maintained in the M-ARCOL by the sole activity of the resident microbiota, with relative percentages of O_2 lower than 2% regardless of the time point and donor (Figure 2A). Once stabilized (days 6 to 10), significantly lower daily gas production was observed in the M-ARILE (Figure 2C), with higher H_2 and lower CO_2 percentages compared to the M-ARCOL. CH_4 was detected only under colonic conditions (Figure 2B). Stabilization of SCFA profiles occurred in 4–6 d in the M-ARILE depending on the individual, compared to only two days in the M-ARCOL for all donors (Figure 3A). After stabilization, SCFA profiles were donor dependent in the ileal model, with an average acetate/propionate/butyrate ratio of 80/17/4% ($\pm 13/10/4\%$). In contrast, in M-ARCOL, SCFA proportions were very similar between donors, with a distinct ratio of 66/24/10% ($\pm 3/3/1\%$) (Figure 3A). The total SCFA concentration (19 versus 134 mM, $P < 0.001$), as well as the main SCFA concentrations, were significantly lower under ileal compared to colonic conditions (Figure 3B). Targeted metabolomic analysis corroborated the HPLC results for SCFAs (Suppl. Figure 3) and highlighted distinct bile acid profiles between the ileum and colon *in vitro* (Figure 4A). All primary bile acids (cholic, chenodeoxycholic, glycocholic and taurocholic acids), as well as five secondary bile acids (glyco-deoxycholic, taurodeoxycholic, deoxycholic, hyodeoxycholic and ursodeoxycholic acids), were found at significantly ($P < 0.0001$) higher levels in the M-ARILE compared to M-ARCOL (Figure 4C). Furthermore, RDA revealed different profiles of untargeted metabolites between M-ARILE and M-ARCOL, mostly driven by fasted and fed states in the ileal model (Figure 5A). Among the 54 metabolites detected by nontargeted metabolomics, 26 were found at significantly ($P > 0.01$) higher amounts in the M-ARILE (e.g., alanine, glutamic acid, inositol and galactose), and only two (phenylacetic acid and octadecadienoic acid) were more abundant in the M-ARCOL (Figure 5C).

Microbiota diversity and composition under ileal versus colonic conditions

In parallel with monitoring metabolic activities, microbiota composition and diversity were followed in the *in vitro* models by qPCR and 16S metabarcoding analyses. The microbiota stabilization in the two models was associated with a decrease in microbial richness and diversity, by comparison with the initial stool suspension (Figure 6A,B). Regarding α -diversity, a stable state was reached at days 4–6 and days 6–8 for the M-ARILE and M-ARCOL models, respectively. From days 6 to 10, more ASVs and significantly greater Shannon index were observed in the ileum compared to colon luminal compartment, while opposite trends were spotted in the mucosal phase (Figure 6C,D). Once stabilized, the total bacterial number was significantly ($P < 0.0001$) lower in the ileum versus colonic conditions in the luminal compartment (median values of 8.3 compared to 9.3 log 16S rDNA copies/mL), while non-significant differences were found for the mucosal phase (Figure 7A,B). The total bacterial decrease in the M-ARILE group was associated with significantly lower amounts of *Bacteroidetes* (Suppl. Figure 4A and 4B) and *Firmicutes* (Suppl. Figure 5A and 5B). In contrast, *γ-Proteobacteria* were more abundant under ileal conditions compared to colonic ones in both the luminal and mucosal compartments (Suppl. Figure 6A and 6B). According to the 16S metabarcoding data, stabilization of the bacterial composition was delayed in the M-ARILE compared with the M-ARCOL and in the mucosal compared to luminal compartments, regardless of the taxonomic level (Suppl. Figure 7A and 7B and Figure 7D). RDA confirmed that a stable state was reached at day 6 in both models (Figure 8B), highlighting separate clustering between ileal and colonic conditions (Figure 8C). This finding indicates that applying ileal or colonic nutritional and physicochemical parameters to the same fecal sample led to markedly different bacterial profiles in the two systems (in both luminal and mucosal microenvironments), with M-ARILE clustering much farther from the initial stool suspension than M-ARCOL. Differential analysis between ileal and colonic conditions revealed a significant enrichment of *Pseudomonadota* and *Thermodesulfobacteriota* phyla, as well as *Clostridiaceae*, *Enterococcaceae*, *Veillonellaceae*, *Enterobacteriaceae* and *Desulfovibrionaceae* families in the M-ARILE (Figure 9A,B). Finally, 14 genera, such as *Clostridium*, *Enterococcus* and *Bacteroides*, were significantly more abundant in the M-ARILE, whereas *Alistipes*, *Ruminococcus* and *Faecalibacterium* were among the 15 most

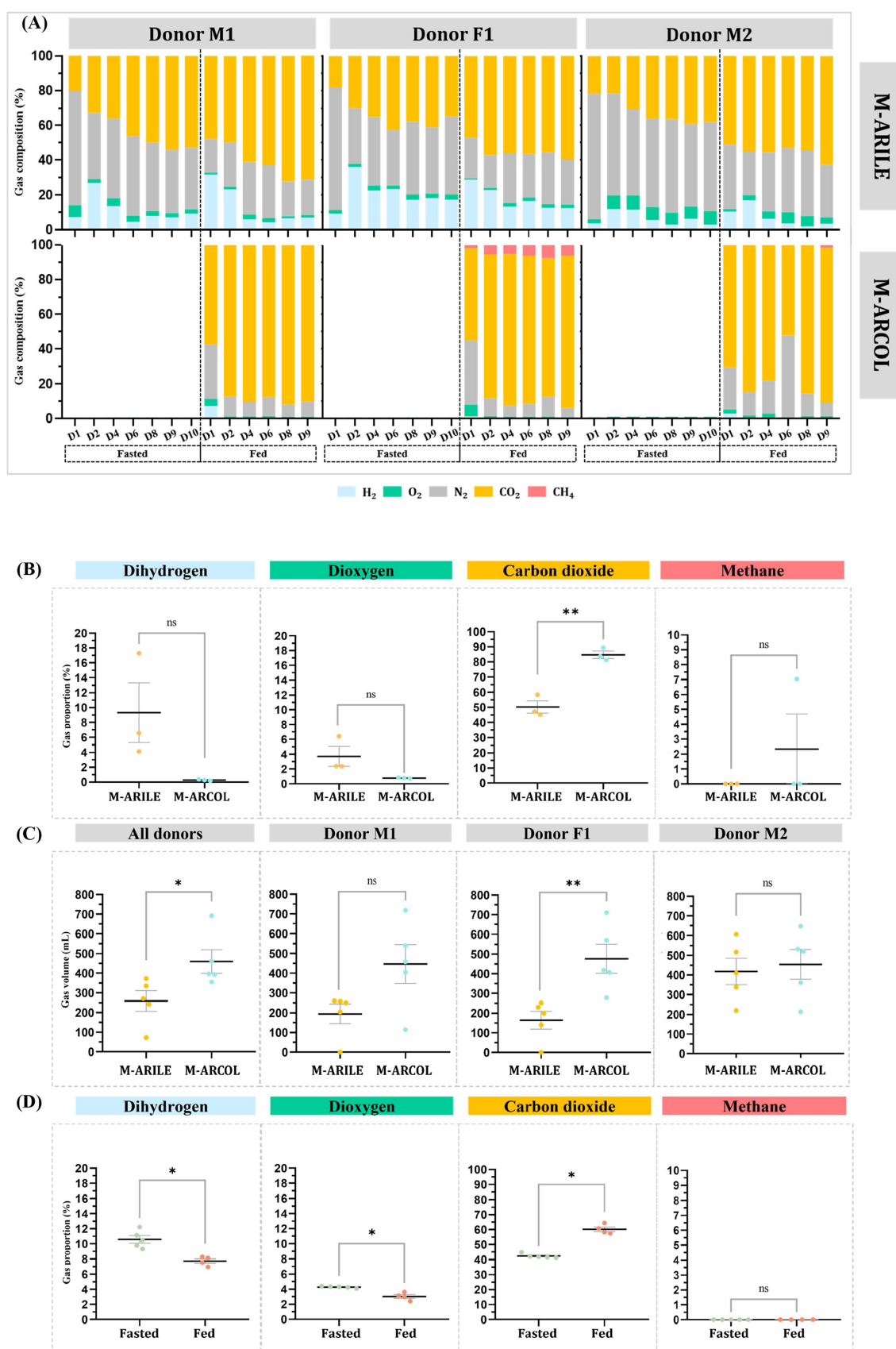


Figure 2. Gas production and composition in the atmospheric phases of M-ARILE and M-ARCOL. Fermentations were run in M-ARILE and M-ARCOL inoculated with fecal samples from three healthy adult donors (M1, F1 and M2). Samples were regularly collected in the atmospheric phase of the bioreactors. Gas composition (in relative percentages) for each donor

(caption on next page)

throughout fermentation in both fasted and fed states (A). Production of H₂, O₂, CO₂ and CH₄ (in relative percentages, mean ± SEM) in M-ARILE vs M-ARCOL during the stabilized days (D6-D10) when all donors are pooled (B). Daily total gas production (in mL, mean ± SEM) during the stabilized days (from D6 to D10) when all donors were pooled and for each individual (C). Production of H₂, O₂, CO₂ and CH₄ (in relative percentages, mean ± SEM) in the M-ARILE during the fasted vs fed state during the stabilized days (D6-D10) when all donors are pooled (D). The significance between the M-ARILE and M-ARCOL results was assessed using an unpaired t test. The significance of differences between fasted and fed states in the M-ARILE was tested with the Mann–Whitney test. ns: not significant, **P* < 0.05 and ***P* < 0.01. H₂: dihydrogen, O₂: dioxygen, N₂: dinitrogen, CO₂: carbon dioxide, CH₄: methane.

abundant genera in the M-ARCOL (Suppl. Figure 9A). Interestingly, non-bacterial populations such as methanogenic *Archaea*, which were exclusively found and maintained in the *in vitro* colonic environment and represented by the *Euryarchaeota* phylum and the *Methanobacteriaceae* family, with *Methanosphaera* genus only (Figure 10A,B and Suppl. Figure 8), were also monitored.

Reproduction of fasted and fed states in the ileal *in vitro* model

Fasted and fed states were implemented in the M-ARILE to simulate repeated influx of food and investigate their influence on microbiome metabolic dynamics. This significantly impacted all fermentation gases in the headspace of the M-ARILE bioreactors, except for methane (Figure 2D). The amounts of O₂ and H₂ were significantly greater under fasted condition than under fed one, whereas opposite trends were observed for CO₂. Feeding status also influenced SCFA profiles (Figure 3A, Suppl. Figure 3B), with increased total SCFA, acetate and propionate concentrations in the fed state, whereas butyrate, isobutyrate and isovalerate were not impacted (Figure 3C, Suppl. Figure 3B). Targeted metabolomic analysis revealed differential clustering of bile acids between the fasted and fed states, in accordance with the different compositions applied between the minimum and rich media in the M-ARILE (Figure 4B, Table 1). Furthermore, 4 out of the 10 bile acids analyzed (glycocholic, taurocholic, glycodeoxycholic and taurodeoxycholic acids) were present in significantly higher amounts (*P* < 0.0001) under fed condition (Figure 4D). Untargeted metabolomics also revealed differential clustering of samples between fasted and fed states (Figure 5B). Among the 54 metabolites identified, 34 were significantly found in higher amounts during the fed state, and only 4 (i.e., methionine 1TMS, phenylacetic acid 1TMS, citrulline 3TMS and spermidine 5TMS) were more abundant in the fasted state (Figure 5D). Regarding microbiota composition, selected populations quantified by qPCR, namely, total bacteria, *Bacteroidetes*, *Firmicutes* and *γ-Proteobacteria*, were not impacted by the feeding status (Figure 7C, Suppl. Figure 4C, Suppl. Figure 5C and Suppl. Figure 6C). Bacterial richness was not affected (Figure 6E), whereas bacterial diversity was significantly increased under fasted condition (Figure 6F). During the stable phase, RDA highlighted different clusters of fed and fasted luminal samples (Figure 8D), in accordance with fluctuations in bacterial profiles observed at all taxonomic levels (Suppl. Figure 7A and 7B and Figure 7D). These findings were supported by differential analysis showing significantly greater abundances of *Verrucomicrobiota* (*Akkermansiaceae* and *Akkermansia* at the family and genus levels) under fasted condition but lower abundances of *Bacteroidota* and *Bacillota* (Figure 9G,H, Suppl. Figure 9D).

Capturing inter-individual variability and specific ileal microenvironments in the M-ARILE

To capture inter-individual variabilities in gut microbes found *in vivo*, M-ARILE and M-ARCOL were inoculated with stool samples from three different healthy adults, two males and one female (M1, F1 and M2). The gas profiles were donor-dependent in both models (Figure 2A). In the M-ARILE, the relative percentage of O₂ during the stabilized phase was three times greater in donor M2 than in the two others, and donor F1 produced the greatest level of H₂. In M-ARCOL, CH₄ was detected throughout fermentation solely for F1 and only at the end of the experiment for M2. CH₄ production in the atmospheric phase of bioreactors can be linked to the presence of methanogenic *Archaea* in both the luminal and mucosal compartments solely for F1 and in two distinct samples from the mucosal phase for M2 (Figure 10 and Suppl. Figure 8). This underlines that the M-ARCOL, but not the M-ARILE, is able to reveal the methane or non-methane producer status of individuals (*Archaea* were not found, most likely because they were

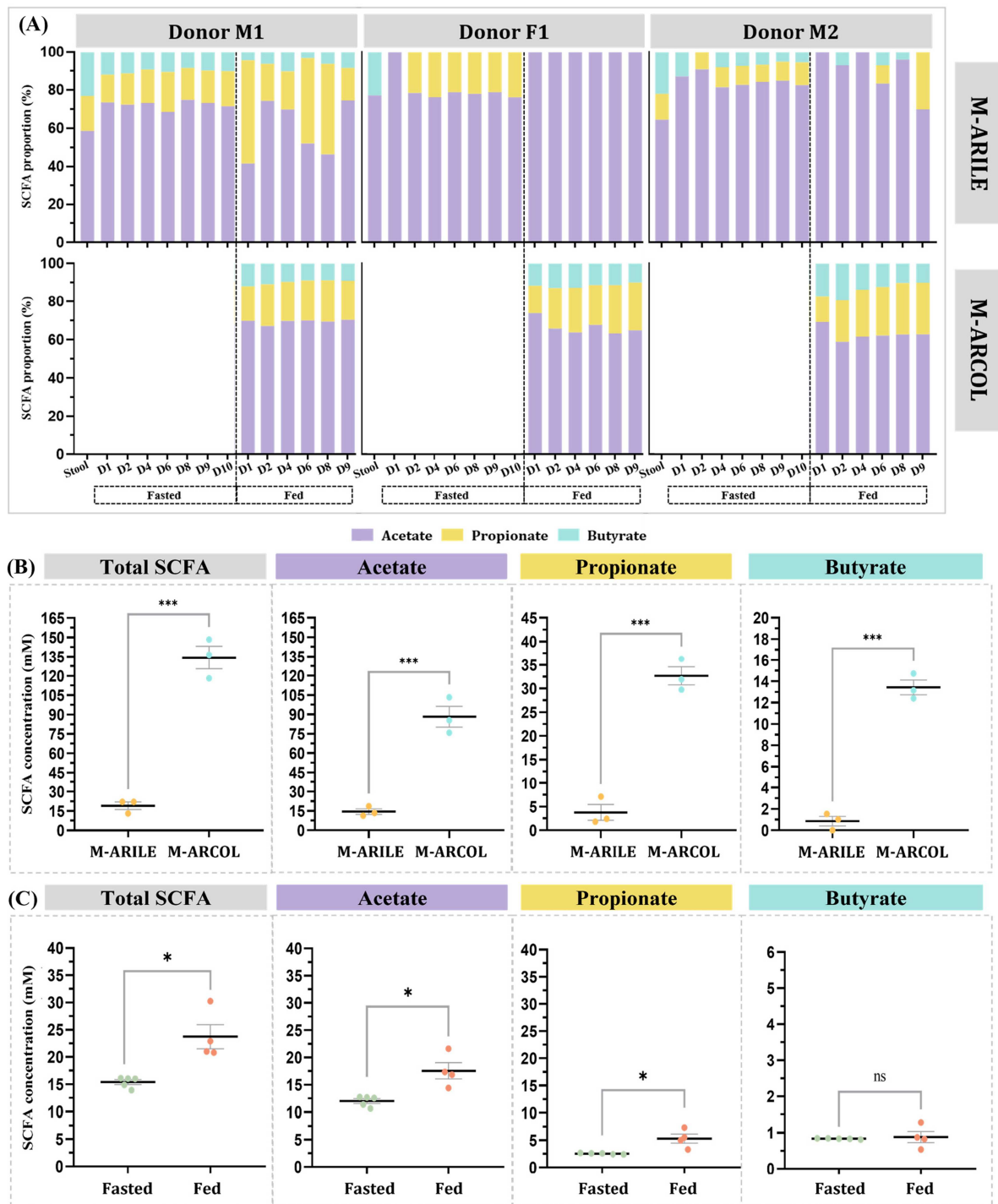


Figure 3. Short-chain fatty acid production in the luminal compartments of M-ARILE and M-ARCOL. Fermentations were run both in M-ARILE and M-ARCOL inoculated with fecal samples from three healthy adult donors (M1, F1 and M2). Samples were collected regularly from the luminal compartments throughout fermentation. The composition of the main SCFAs, i.e., acetate, propionate and butyrate (in relative percentages), were measured by HPLC-DAD for each donor in both fasted and fed states (A). Concentrations of acetate, propionate, butyrate and total SCFAs (in mM, mean \pm SEM) in M-ARILE vs those in M-ARCOL during stabilized days (D6-D10), with all donors pooled (B). Concentrations in acetate, propionate, butyrate and total SCFAs (in mM, mean \pm SEM) in M-ARILE under fasted vs fed state during the stabilized days (D6 - D10) with all donors pooled (C). The significance between the M-ARILE and M-ARCOL results was assessed using an unpaired t test. The significance of differences between fasted and fed states in the M-ARILE was tested with the Mann-Whitney test. ns: not significant, * $P < 0.05$ and *** $P < 0.001$. SCFA: short-chain fatty acid.

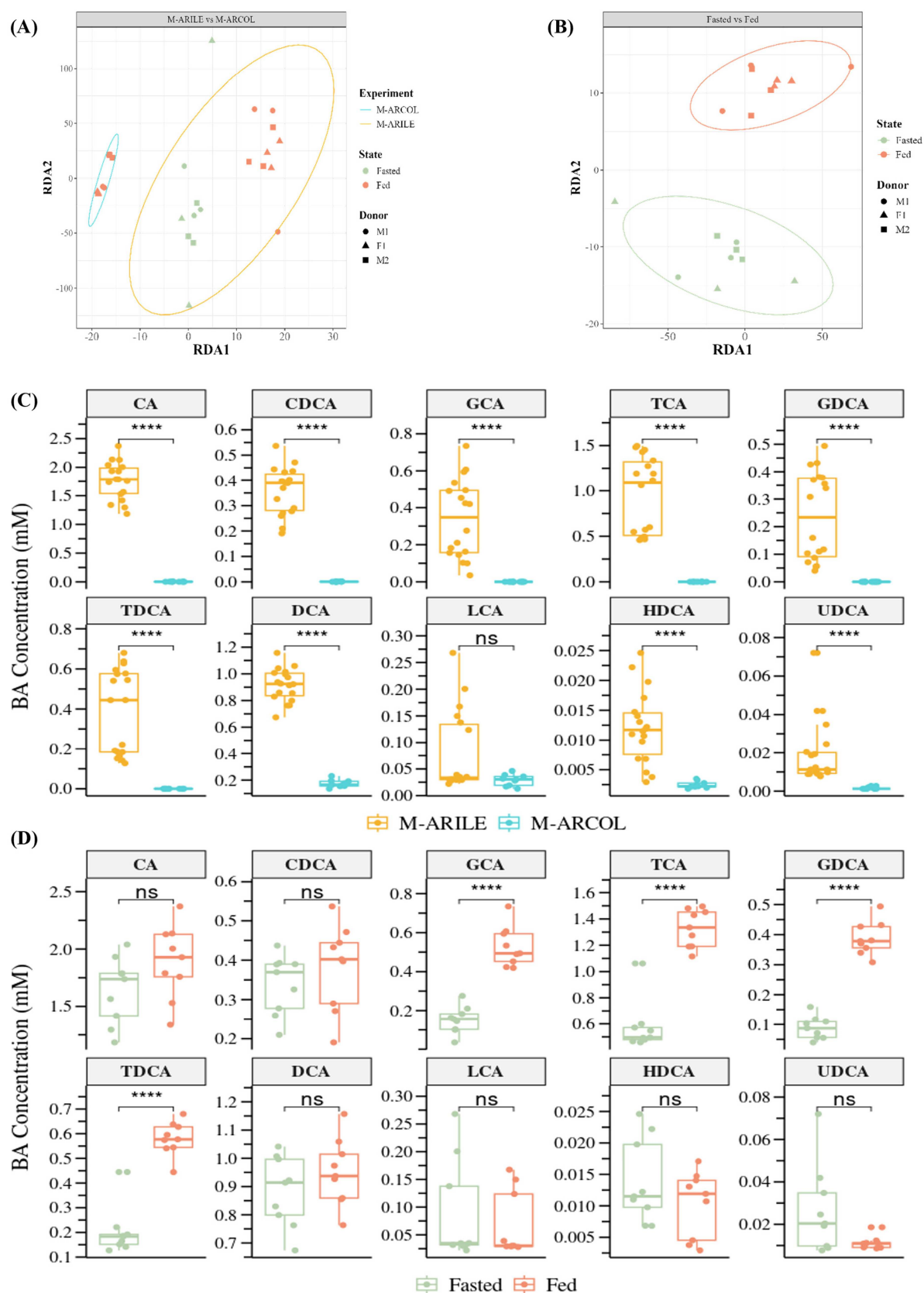


Figure 4. Bile acid profiles under different experimental conditions (M-ARILE versus M-ARCOL) and nutritional statuses (fasted versus fed). Fermentations were run in M-ARILE and M-ARCOL inoculated with fecal samples from three donors (M1, F1 and M2). The main bile acid concentrations were determined via targeted metabolomic analysis using liquid chromatography coupled with tandem mass spectrometry (LC-MS/MS). Only the results obtained in the stabilized period, (caption on next page)

i.e., from day 7 to day 9, are presented. Redundancy analysis (RDA), two-dimensional plot visualizations with Euclidean distance excluding the donor effect, highlights the impact of the experimental conditions, i.e., M-ARILE *versus* M-ARCOL (A) and fasted *versus* fed states in the M-ARILE (B). Concentrations of the main bile acids (in mM, mean \pm SEM, $n = 3$ donors) in the M-ARILE and the M-ARCOL (C). Concentrations of main bile acids (in mM, mean \pm SEM, $n = 3$) in the M-ARILE under fasted *versus* fed state (D). Statistical analyses were performed using the Wilcoxon test. ns: not significant; **** $P < 0.0001$. BA: bile acid, CA: cholic acid, CDCA: chenodeoxycholic acid, DCA: deoxycholic acid, GCA: glycocholic acid, GDCA: glycodeoxycholic acid, HDCA: hyodeoxycholic acid, LCA: lithocholic acid, TCA: taurocholic acid, TDCA: taurodeoxycholic acid, and UDCA: ursodeoxycholic acid.

under the detection limit, in the fecal samples from the three donors). Regarding SCFAs, profiles were very similar between donors in the M-ARCOL, while a wide inter-individual variability was observed in the M-ARILE (Figure 3A). For example, donor F1 exhibited SFA profiles clearly different from those of M1 and M2, both in the initial stool and in the M-ARILE with no butyrate production. The RDA of bacterial β -diversity clearly revealed a donor-dependent clustering of samples in both models (Figure 8A), highlighting that they were efficient at capturing *in vivo* inter-individual variabilities in bacteria and *Archaea* (Figure 7D, Figure 10, Suppl. Figure 7 and Suppl. Figure 8). For instance, in M-ARILE, *Acidaminococcaceae* were found in donor M2, while *Bacillaceae* were detected only in donor M1. Similarly, in M-ARCOL, *Rikenellaceae* were among the most abundant populations only in donor M1, and *Desulfovibrionaceae* were mostly found in donor F1.

As previously described for M-ARCOL¹⁶ and confirmed in the present study (Figure 8F), the connection of a mucin bead compartment to the main bioreactors allowed us to distinguish luminal microbiota from mucus-associated microbiota in the ileal compartment (Figure 8E). The number of ASVs was higher in the mucus phase of the M-ARILE group than in the luminal phase (Figure 6C), while opposite trend was found for the total bacterial load (Figure 7B). Distinct profiles were observed between the two microenvironments for bacteria (Figure 7D and Suppl. Figure 7A and 7B) and/or *Archaea* (Figure 10 and Suppl. Figure 8) at all taxonomic levels in the M-ARILE and M-ARCOL. Globally, *Bacillota* (e.g., *Lachnospiraceae* and *Ruminococcaceae*) and *Thermodesulfobacteriota* (e.g., *Desulfovibrionaceae*) were more abundant in the mucosal phase than in the luminal phase. Concerning the non-bacterial fraction, more *Archaea* ASVs were found in the mucosal compartment than in the luminal compartment of the M-ARCOL. Lastly, differential analysis revealed that at the phylum level, all bacterial populations were similarly impacted between the M-ARILE and M-ARCOL in the luminal and mucosal compartments (Figure 9C,E). In contrast, at the family level, *Peptostreptococcaceae*, *Butyricicoccaceae* (and *Butyricoccus* at the genus level), *Enterobacteriaceae* (and *Enterobacteriaceae_genus*) and *Sutterellaceae* were significantly increased in the M-ARILE compared with the M-ARCOL, only in the luminal compartment but not in the mucin beads (Figure 9D,F, Suppl. Figure 9B and 9C).

Multivariate analysis for findings associations between microbiota composition and functionality

Spearman correlations were performed to assess the correlation between bacterial composition and SCFA or bile acid concentrations in the M-ARILE and M-ARCOL (Figure 11). The most striking result was that the correlations were widely dissimilar between the ileal and colonic models for both SCFA and bile acids. In the M-ARILE, *Enterococcaceae* were positively correlated with propionic acid, GCDCA and GUDCA (Figure 11A,C, $P < 0.05$), while *Marinifilaceae* were negatively correlated with cholic acid and GCDCA (Figure 11A,C, $P < 0.05$). In addition, *Enterobacteriaceae* were positively correlated with HDCA ($P < 0.01$), and UDCA was negatively correlated ($P < 0.05$) with *Prevotellaceae* and positively correlated with *Clostridiaceae* (Figure 11C). Interestingly, negative correlations were detected between all the genera and SCFAs, except for HA, which was strongly positively correlated with almost all the bacteria (Figure 11B, $P < 0.001$). In M-ARCOL, *Christensenellaceae* and *Prevotellaceae* were positively correlated with acetate and UDCA, respectively (Figure 11A,C, $P < 0.05$). UDCA was positively correlated with *Prevotella*, *Eubacterium* and *Alloprevotella* (Figure 11D, $P < 0.001$). Finally, *Ruminococcaceae* (and *Ruminococcus*) were negatively correlated with all bile acids in the two models.

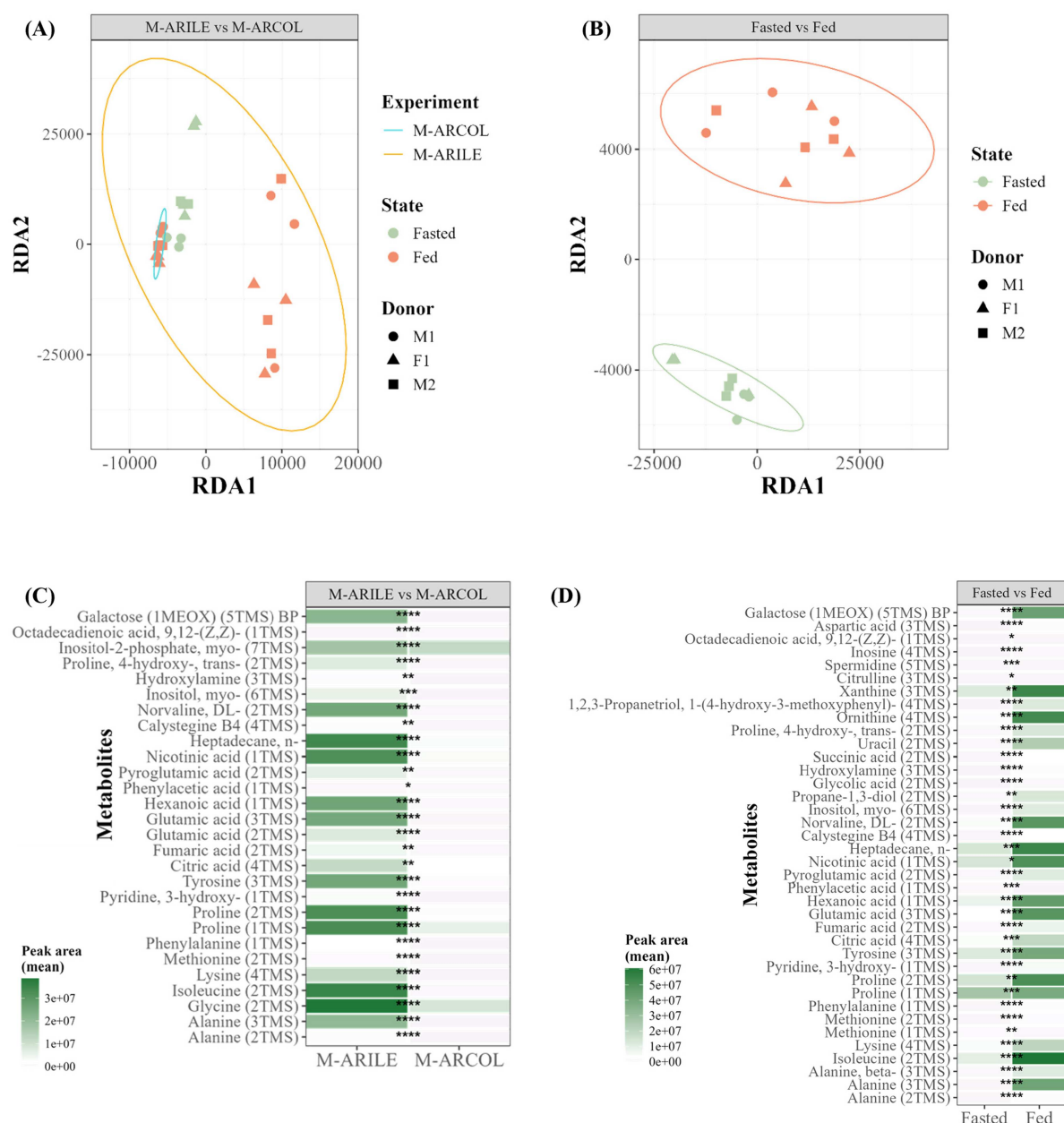


Figure 5. Effect of experimental conditions (M-ARILE versus M-ARCOL) and nutritional statuses (fasted versus fed) on metabolite production as assessed by untargeted metabolomics. Fermentations were run in M-ARILE and M-ARCOL inoculated with fecal samples from three donors (M1, F1 and M2). Polar luminal metabolite profiling was performed using gas chromatography coupled with a quadrupole time-of-flight (qTOF) mass spectrometer configured in full-scan mode. Only significant results obtained in the stabilized period, i.e., from day 7 to day 9, are presented. Redundancy analysis (RDA), two-dimensional plot visualizations with Euclidean distance excluding the donor effect, highlights the impact of the experimental conditions, i.e., M-ARILE versus M-ARCOL (A) and fasted versus fed states in the M-ARILE (B). Heat map visualization of significant changes in untargeted metabolite composition (in peak area, mean, $n = 3$ donors) in M-ARILE versus M-ARCOL (C) and fasted versus fed states in the M-ARILE (D). Statistical analyses were performed using the Wilcoxon test. ns: not significant; * $P < 0.05$, ** $P < 0.01$, *** $P < 0.001$ and **** $P < 0.0001$.

Validation of the newly developed ileal model through in vitro-in vivo comparisons

In order to validate the newly developed *in vitro* M-ARILE model, its microbiota composition and metabolic profiles from the stabilization phase were compared to those from *in vivo* data (Tables 3 and 4). The total SCFA, acetate and propionate concentrations (Table 3) were fully in accordance with the *in vivo* data from the human ileum. Only butyrate concentrations were lower than those observed *in vivo* (0.9

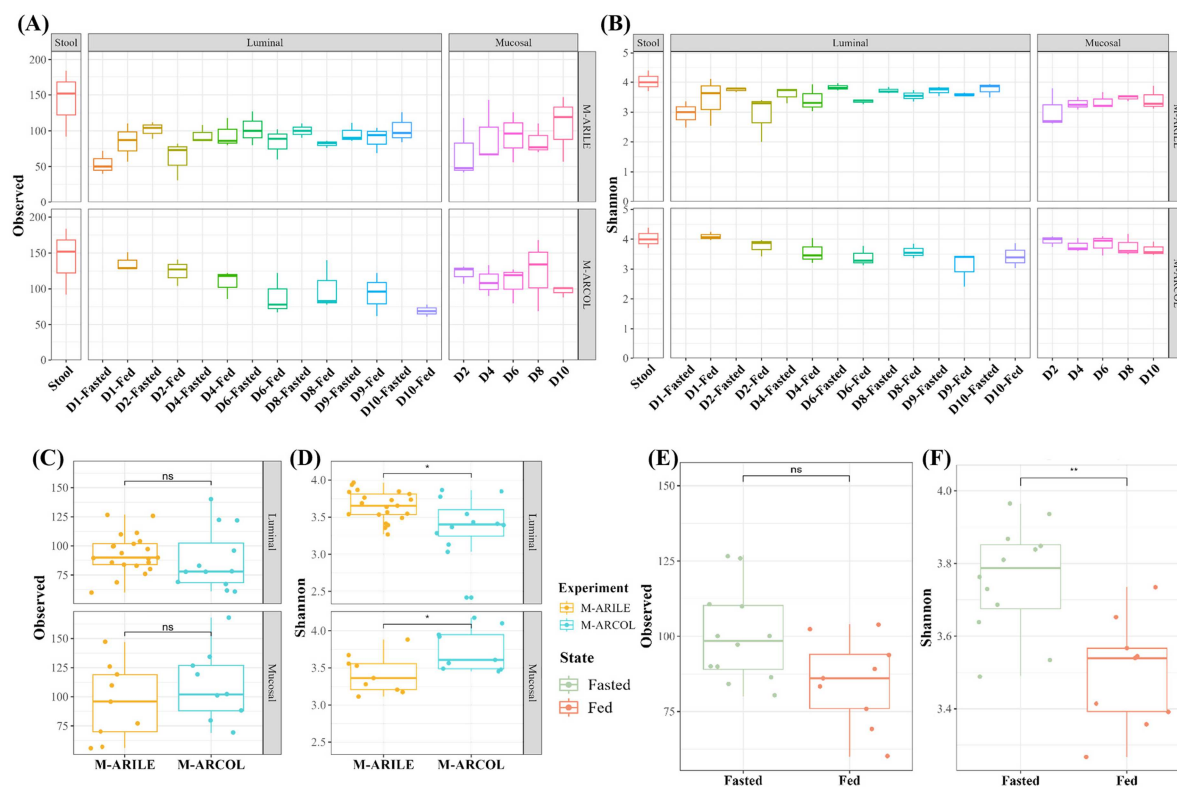


Figure 6. Alpha-diversity of bacterial communities in the M-ARILE and M-ARCOL models. M-ARILE and M-ARCOL were inoculated with stool samples from three healthy adults and run under continuous fermentation for 10 d. Samples were collected daily in the luminal compartment of M-ARCOL and twice a day in the M-ARILE ('fasted' and 'fed'). Mucin beads were collected every two days (mucosal compartment). The compositions of the lumen and mucus-associated microbiota were determined by 16S metabarcoding, and α -diversity indices were calculated at the ASV level. The observed ASVs (A) and the Shannon index (B) are represented as box plots throughout fermentation ($n = 3$). Stabilized values (from D6 to D10) are compared between M-ARILE and M-ARCOL for the observed ASVs (C) and the Shannon index (D). For the M-ARILE, a comparison between the fasted and fed states is also given (E and F). Statistical differences were tested via the Wilcoxon test and indicated by ns: not significant, * ($P < 0.05$), and ** ($P < 0.01$).

versus 2.3–13.7 mM). SCFA concentrations and ratios showed a similar evolution from the ileum towards the colon as that of the *in vivo* situation. The proportions of O_2 , H_2 and CH_4 (Table 3) were in line with those found in the human ileum, whereas the percentage of CO_2 *in vitro* was much higher than that *in vivo* (50.3 versus 17.5%). Compared with the *in vivo* data, all fermentation gases—except for H_2 —showed a similar evolution from the *in vitro* ileum to the colon. In addition, the most abundant phyla or families found *in vitro* in both the luminal and mucosal compartments of the M-ARILE were compared to *in vivo* data collected in the human ileum by aspiration or biopsy, respectively. Thirty-five families were described in the human ileum, irrespective of the sampling location (Table 4). In M-ARILE, 19 were recovered, including 11 in the same compartments *in vitro* and *in vivo*. Among the families not recovered in the M-ARILE but described in humans, only five were reported in more than one study, including *Fusobacteriaceae*, *Streptococcaceae* and *Lactobacillaceae*. In contrast, two phyla (*Actinobacteriota* and *Bdellovibrionota*) and three families (*Bacillaceae*, *Marinifilaceae* and *Erysipelotrichaceae*) were found in the M-ARILE but not *in vivo* (Table 4). Taken together, those *in vitro-in vivo* comparisons validated our newly developed ileal model, both at the microbiota function and composition levels.

Discussion

The small intestine comprises crucial regulatory functions for nutrient absorption, energy metabolism and immune response. However, there is a knowledge gap regarding the role of the residing microbiota in modulating these functions and thereby shaping health status.⁵⁴ As accessibility to the human ileum in

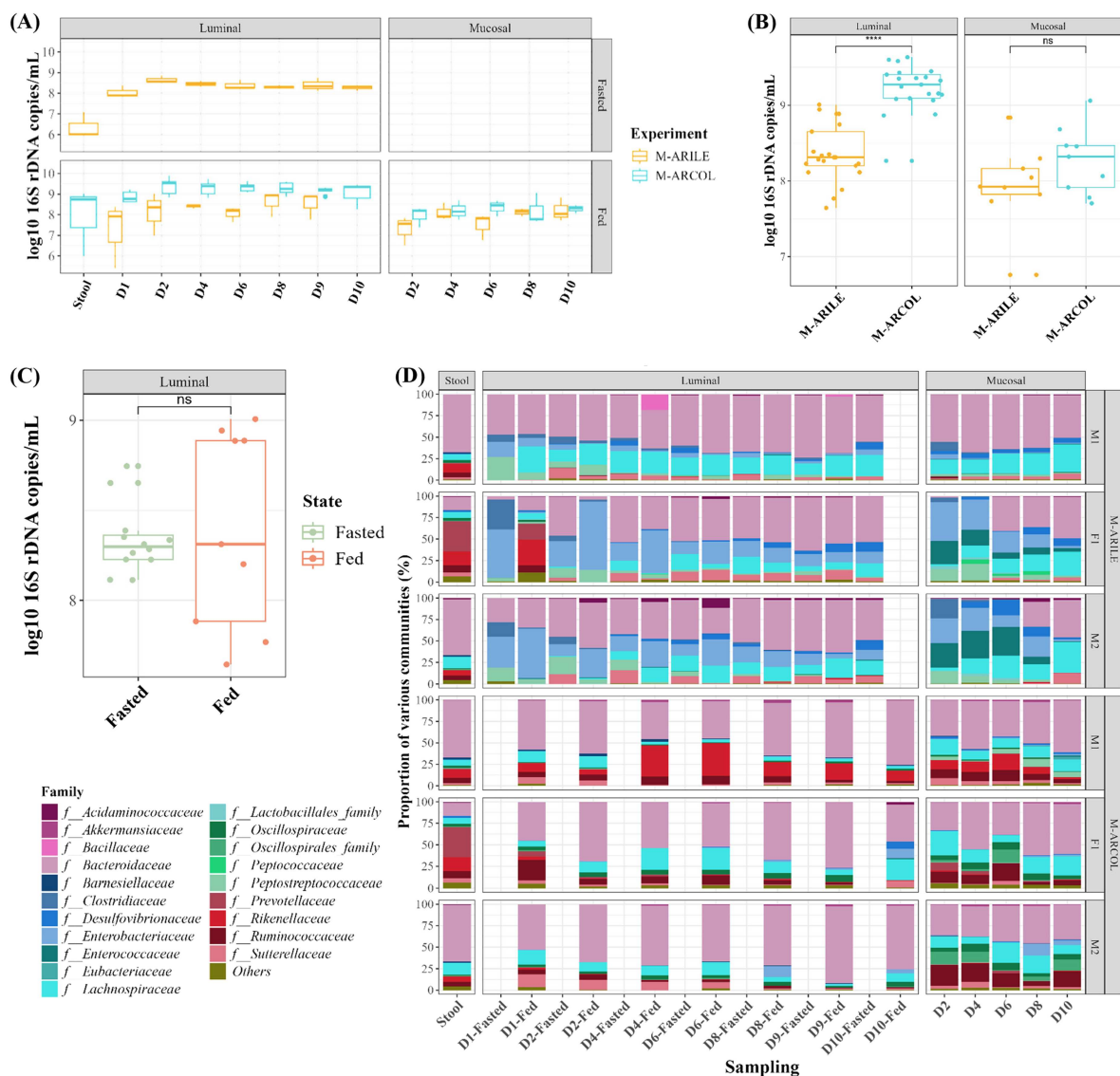


Figure 7. Lumen and mucus-associated bacteria in M-ARILE and M-ARCOL. M-ARILE and M-ARCOL were inoculated with stool samples from three healthy adults (M1, F1 and M2) and run under continuous fermentation for 10 d. The composition of the lumen and mucus-associated microbiota was determined via 16S metabarcoding, and total bacteria were quantified via qPCR. The number of total bacteria is represented using box plots (in 16S rDNA copies/mL or/g) throughout fermentation in the luminal and mucosal compartments of both *in vitro* models. Fasted and fed states are separated in the M-ARILE in the luminal phase (A). During the stabilized period only (i.e., from D6 to D10), total bacteria were compared between M-ARILE and M-ARCOL (B) and between fasted and fed states in the M-ARILE (C). The relative abundances of the main bacterial populations are given for each donor at the family (D) level in the M-ARILE (top) and M-ARCOL (bottom) experiments. Statistical differences were tested by the Wilcoxon test and are indicated by ns: not significant and **** ($P < 0.0001$). No significant difference was found between sampling days for each experimental condition (A).

clinical studies is challenging and in view of the 3R principle to reduce, refine and replace animal research⁵⁵, we aimed to develop and validate a new *in vitro* model for studying the human ileum microbiome.

The newly developed M-ARILE uniquely features the main physicochemical (pH, transit time, bile acid profiles, and oxygen level), mechanical (steering adjustment to mimic reduced motility during the sleeping phase), nutritional (availability of nutrients associated with fed and fasted states) and microbial (lumen and mucus-associated bacteria and *Archaea*) parameters of the human ileum ecosystem. The model has been validated in terms of microbiota composition and main metabolic activities (gas and SCFA production) compared to *in vivo* data in humans (Tables 3 and 4). Such an in-depth *in vitro-in vivo* comparison

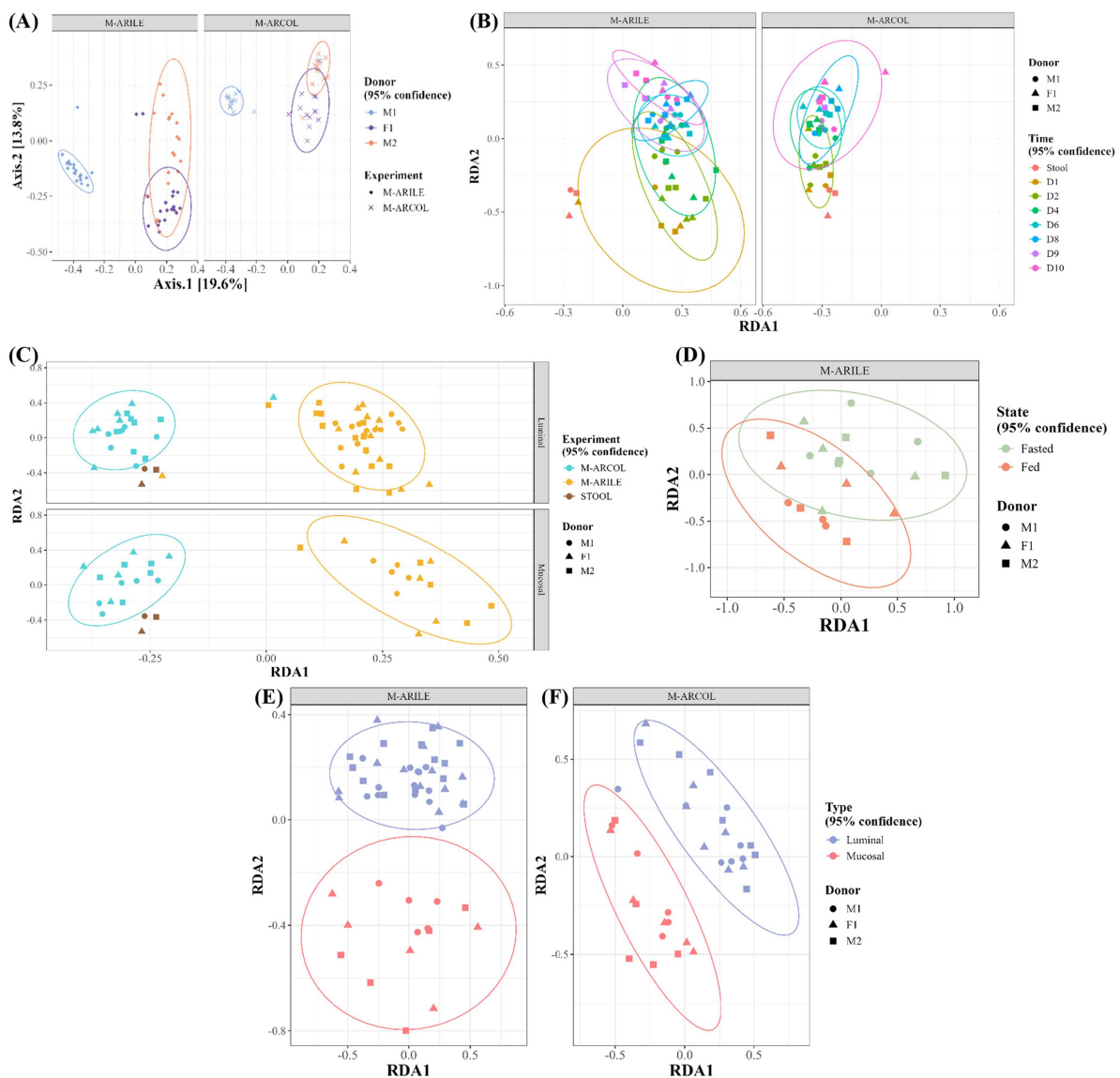


Figure 8. Beta diversity of bacterial communities in the M-ARILE and M-ARCOL models. M-ARILE and M-ARCOL were inoculated with stool samples from three healthy adults (M1, F1 and M2) and run under continuous fermentation for 10 d. The composition of the lumen and mucus-associated microbiota was determined via 16S metabarcoding, and β -diversity analysis was performed at the ASV level. PCoA analysis of bacterial diversity reveals a significant donor effect (A). Redundancy analysis (RDA), two-dimensional plot visualizations of β -diversity with Bray–Curtis distance excluding the donor effect, highlights the impact of the day of fermentation (B), experiment (C), fasted and fed states (stabilized period, i.e., from D6 to D10) (D) and microenvironment (i.e., luminal *versus* mucosal) in the M-ARILE (E) and the M-ARCOL (F).

has not yet been performed during the development of other human gut models integrating the ileal microbiota (Table 5), namely, TSI, TIM–1 and M-SHIME.^{12–15} Another unique feature of the M-ARILE is its ability to maintain anaerobiosis without flushing with N₂ (unlike TIM–1 and M-SHIME), relying on the microbiota's own metabolic activities to lower oxygen levels. This offers the great advantage of allowing the measurement of fermentation gases in the headspace. Compared to the M-ARILE model, the TSI model is a very simple batch model in which the microbiota is integrated using a consortium of 7 bacteria,¹³ far from the diversity and complexity of the human ileum microbiota.⁵⁶ The TIM–1 and M-SHIME models, both inoculated with fecal samples or ileostomy effluents, exhibit more similar levels of complexity compared to the M-ARILE model. In contrast to our model, those two *in vitro* systems have the advantage of being multicompartmental (simulating the entire digestive tract for the M-SHIME). In addition, M-SHIME^{14,15} and M-ARILE are the only ones that distinguish lumen from mucus-associated microbes,

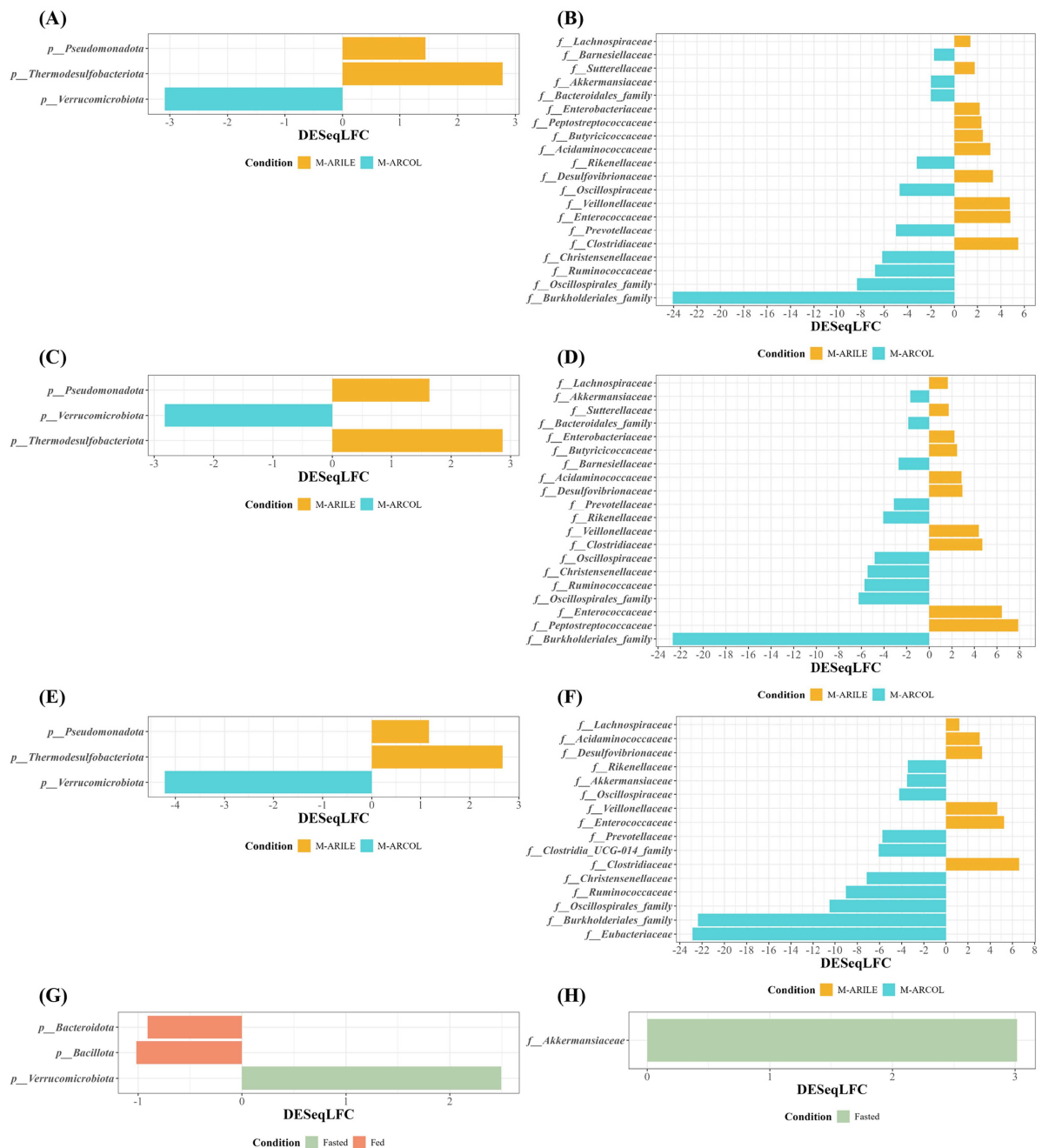


Figure 9. Differential analysis of the impact of experimental conditions and fasted *versus* fed state on bacterial composition at the phylum and family levels. Samples were regularly collected in both the luminal and mucosal compartments of the M-ARILE and the M-ARCOL models during fermentation, and only the results of stabilized days are given (D6-D10). Differential analysis highlights bacterial populations significantly impacted by experimental conditions, i.e., M-ARILE compared to the M-ARCOL, at the phylum and family level respectively, considering the two microenvironments together (A and B) or focusing on the luminal (C and D) or mucosal (E and F) compartment. The impact of fasted *versus* fed state is also specified in the M-ARILE (G and H). The results are significantly different with at least one method among the three tested (DeSeq2, Metacoder and MetagenomeSeq R-analysis).

enabling a more physiological restitution of ileal microenvironments^{57,58} and a greater capture of bacterial diversity from the fecal microbiome^{59–61}. In particular, the M-ARILE mucosal compartment effectively preserved *Bacillota* bacteria like *Lachnospiraceae*^{48,62} as well as mucin-degrading taxa from *Enterobacteriaceae* family.^{9,63} In addition, this *in vitro* study provides useful insights into human luminal and mucosal ileal microbes, that have been poorly studied *in vivo*. In particular, the *Actinobacteriota* and *Bdellovibrionota* phyla, as well as the *Bacillaceae*, *Erysipelotrichaceae* and *Marinifilaceae* families, were

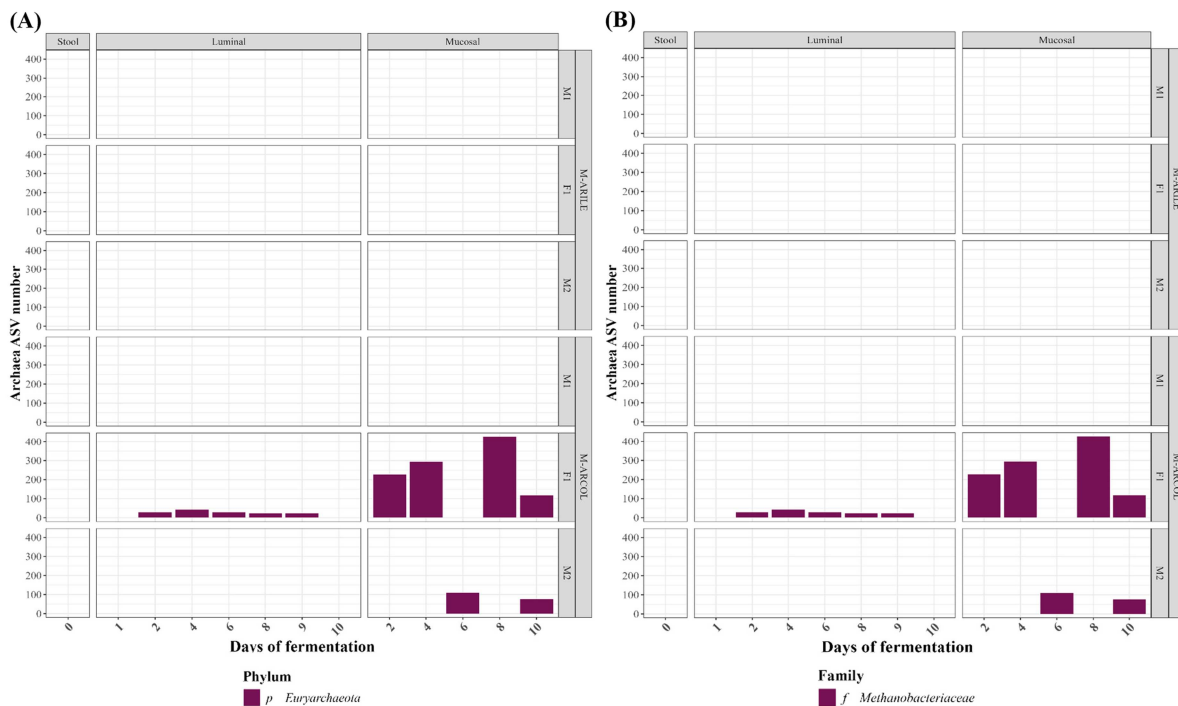


Figure 10. Lumen and mucus-associated *Archaea* in M-ARILE and M-ARCOL. M-ARILE and M-ARCOL were inoculated with stool samples from three healthy adults (M1, F1 and M2) and run under continuous fermentation for 10 d. The composition of the lumen and mucus-associated microbiota was determined via 16S metabarcoding. The ASV numbers of archaeal populations are represented for each donor at the phylum (A) and family (B) levels.

found *in vitro* but not in humans, opening new fields of investigation regarding potential undescribed small intestinal microbes. On the contrary, *Lactobacillaceae*, *Fusobacteriaceae* and *Streptococcaceae* were undetected in the M-ARILE, or in the initial inocula, though found *in vivo*.^{9,49,52,53} These bacteria are commonly associated with the human oral microbiome that can colonize the lower gastrointestinal tract, even in healthy individuals.¹⁰ In future developments, this gap might be filled by adding to the M-ARILE a human artificial saliva containing the lacking populations.⁶⁴ The absence of butyrate-producing *Fusobacteriaceae*, recently identified as part of the core small intestine microbiota,^{56,65} may explain the lower butyrate levels found *in vitro* compared to *in vivo*.^{7,44}

Another validation criterion for the M-ARILE was the ability to obtain an ileum microbiome that clearly differentiates from that of the colon. We therefore conducted simultaneous fermentation experiments in the M-ARILE and M-ARCOL, which solely mimic the human large intestine.^{16,17,66} This approach also allowed us to confirm or obtain some useful insights into the differences between the human ileal and colonic ecosystems. Importantly, as described above, we showed for the first time that by applying ileal physicochemical and nutritional parameters to fecal microbes, a shift to ileum-like profiles can be reached, both at the structural and functional levels. This approach using fecal samples was favored in this study (instead of a bacterial consortium) to retain in M-ARILE the complexity and interindividual variabilities found *in vivo*. Analysis of bacterial β -diversity revealed greater differences between the M-ARILE and the initial fecal samples than between the M-ARCOL and the stool samples.⁴⁷ This finding is expected since the colon and feces samples clearly exhibit similar physicochemical (e.g., pH and bile salt concentrations) and nutritional (e.g., availability of fermentable carbohydrates) parameters than the ileum and feces samples do.⁶⁷ M-ARILE displayed lower total bacterial loads than in the M-ARCOL, with higher colonization in the luminal phase compared to the mucosal phase, which is also in line with *in vivo* data.^{6,62} This is related to the colonization of the intestinal mucus layer by more specialized bacteria that are able to adhere to and use mucin glycoproteins as main nutrients.^{62,68} Patrascu et al. demonstrated that the bacterial ecosystem in the human ileal mucosa harbors host-glycan-degrading glycoside hydrolases belonging to the carbohydrate-active enzymes (CAZymes) family.⁶⁹ As described *in vivo*, *Enterobacteriaceae* and *Veillonellaceae* dominated in the M-ARILE, while *Akkermansiaceae* and

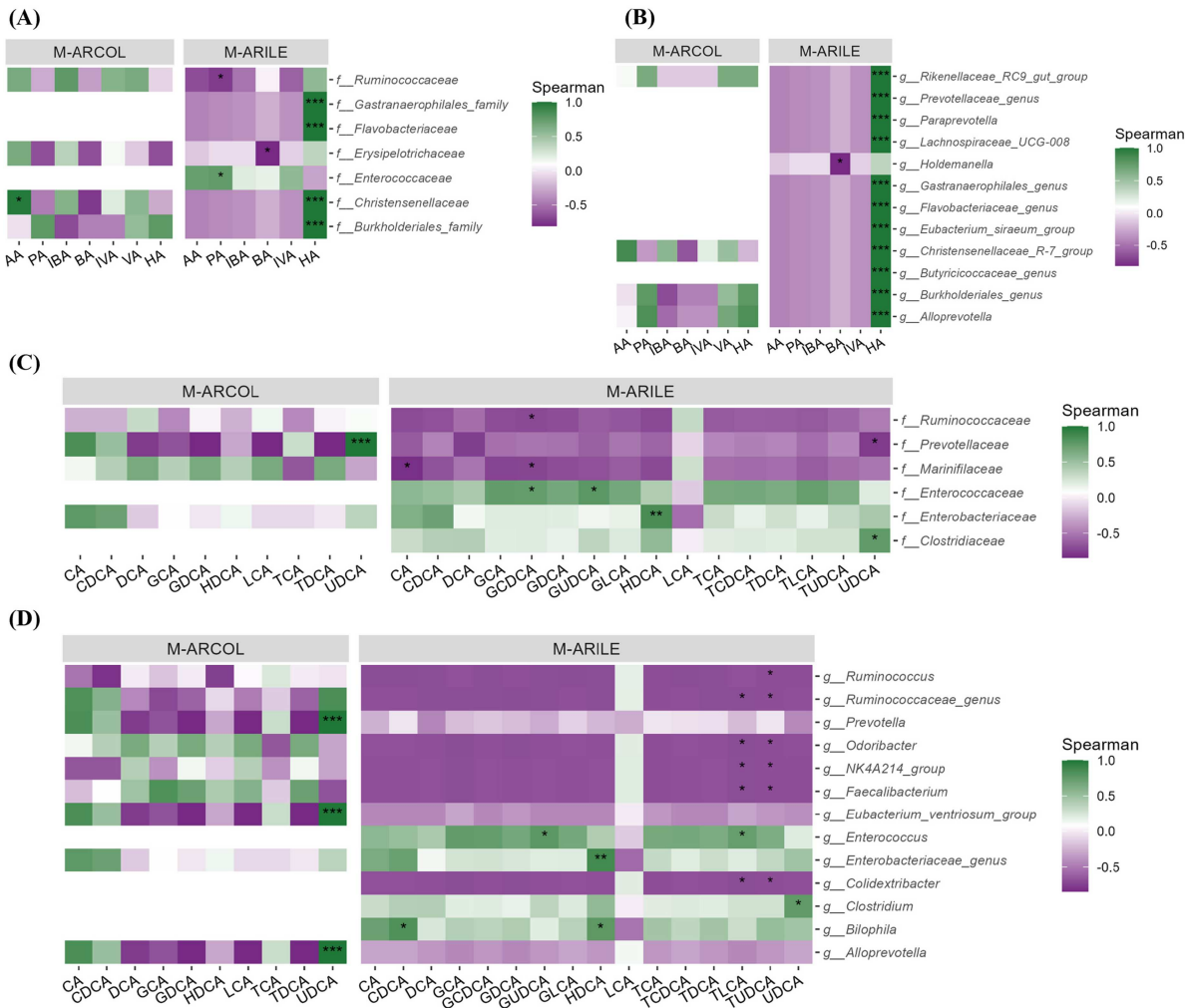


Figure 11. Spearman correlation between microbiota composition and SCFA/bile acid concentrations at the family and genus levels. Samples were regularly collected in the luminal compartments of the M-ARILE and the M-ARCOL during fermentation. The microbiota composition and SCFA/bile acid concentrations were analyzed via 16S metabarcoding and targeted GC–MS/MS or LC–MS/MS, respectively. Only the results for stabilized days are presented (D8 and D9). Spearman correlations between microbiota composition and SCFA (A and B) and bile acid concentrations (C and D) are given at the family (A and C) and genus (B and D) levels. The green color indicates a positive correlation, while purple color denotes a negative one. The color shading indicates the magnitude of the association. Asterisks indicate p value significance, with * ($P < 0.05$), ** ($P < 0.01$) and *** ($P < 0.001$). AA: acetic acid, BA: butyric acid, CA: cholic acid, CDCA: chenodeoxycholic acid, DCA: deoxycholic acid, GCA: glycocholic acid, GCDCA: glycochenodeoxycholic acid, GDCA: glycodeoxycholic acid, GLCA: glycolithocholic acid, GUDCA: glyoursodeoxycholic acid, HA: hexanoic acid, HDCA: hyodeoxycholic acid, IBA: isobutyric acid, IVA: isovaleric acid, LCA: lithocholic acid, PA: propionic acid, TCA: taurocholic acid, TCDA: taurodeoxycholic acid, TDCDA: taurochenodeoxycholic acid, TLCA: tauroolithocholic acid, TUDCA: taoursodeoxycholic acid, UDCA: ursodeoxycholic acid and VA: valeric acid.

Prevotellaceae were more prevalent in the M-ARCOL.^{6,56} In the ileal mucosal environment, *Ruminococcaceae* were more abundant, while *Sutterellaceae* were mainly found in the luminal phase, again in line with *in vivo* data.^{9,52,53}

Regarding microbial activities, both non-targeted metabolomics and spearman correlations between bacterial composition and main gut metabolites (SCFAs and bile acids) highlighted very distinct profiles between the M-ARILE and M-ARCOL experiments, supporting the existence of different metabolic pathways in the ileal and colonic ecosystems.^{44,70} In accordance with *in vivo* data, gas and SCFA production was highly impacted by ileal *versus* colonic conditions *in vitro*. Oxygen level was higher in the M-ARILE than in M-ARCOL, reflecting the less anaerobic conditions found in the human ileum that fosters microaerophilic bacteria like *Enterobacteriaceae*.^{4,54,71} Of note, the oxygen gradient that also exists

Table 3. Validation of the M-ARILE model through *in vitro-in vivo* comparisons regarding microbial metabolic activities.

In vitro mean results in the M-ARILE during the stabilized period (with extreme values depending on the donor) were compared to *in vivo* data in the ileum of healthy human adults (based on literature review), regarding both concentrations or relative percentages of gas and/or SCFAs and direction of variations between ileal and colonic conditions (↗: increase in the M-ARILE, ↘: decrease in the M-ARILE).

Metabolic activity		M-ARILE	<i>In vivo</i> (ileum)	Correlation	M-ARILE vs M- ARCOL	<i>In vivo</i> (ileum vs colon)	Validation	References
SCFA concentrations (mM)	Total SCFA	19.1 (13.2–22.1)	11.7–81.6	✓	↘	↘	✓	[7,44]
	Acetate	14.5 (11.4–18.6)	7.9–64.6	✓	↘	↘	✓	
	Propionate	3.8 (1.8–7.1)	1.5–3.3	✓	↘	↘	✓	
	Butyrate	0.9 (0–1.5)	2.3–13.7	✗	↘	↘	✓	
SCFA proportions (%)	Acetate	78.9 (63.9–87.9)	62.2–78.5	✓	↗	↗	✓	[7,44]
	Propionate	16.7 (9.7–28.26)	4.7–11.8	✗	↘	↘	✓	
	Butyrate	4.3 (0–7.8)	16.8–18.1	✗	↘	↘	✓	
	CH ₄	0	0	✓	↘	↘	✓	
Gas composition (%)	CO ₂	50.3 (44.8–53.7)	6–17.5	✗	↘	↘	✓	[45,46]
	O ₂	3.7 (2.3–6.4)	5–41	✓	↗	↗	✓	
	H ₂	9.3 (4.1–17.3)	0.3–3.5	✗	↗	↘	✗	
	Redox	–237 mV	ND	/	↗	ND	/	

✓: *in vitro* results are in accordance with *in vivo* data, ✗: *in vitro* and *in vivo* data are not in accordance, /: no conclusion can be done due to lack of *in vivo* data. CH₄: methane, CO₂: carbon dioxide; H₂: dihydrogen, M-ARILE: Mucosal Artificial Ileum; M-ARCOL: Mucosal Artificial Colon; ND: no *in vivo* data; O₂: dioxygen; SCFA: short-chain fatty acid.

from the microaerophilic small intestinal lumen towards the highly vascularized oxygen-rich subepithelial mucosa was not reproduced in the M-ARILE.⁷² Methane was not detected under ileal conditions, as well as methanogenic *Archaea*, while both were found under colonic conditions *in vitro* and *in vivo*.⁷³ The absence of *Archaea* under small intestinal conditions may be linked to the faster transit time^{74,75} or the higher bile acid concentrations impacting their viability.⁷⁶ Since only one study previously addressed methanogenic *Archaea* in human ileal samples,⁷⁷ the present study thus provides pioneering data on this non-bacterial fraction of the human gut microbiome. H₂ levels were also relatively high in the M-ARILE, matching the increased abundance of H₂-producing bacteria such as *Bacteroides* and *Clostridium*⁶ and/or the relatively low abundance of H₂ re-user like methanogenic *Archaea*. In line with *in vivo* data, SCFA concentrations were also lower in the M-ARILE due to the shorter transit time and/or lower bacterial load, which limit microbial fermentation.⁷⁰ Butyrate production was also lower under ileal condition than under colonic one because of the reduced abundance of *Firmicutes*.⁷⁸ Bile acid profiles were also followed in the *in vitro* models, reflecting both the composition of nutritive media and the metabolic activities occurring during fermentation. In accordance with human digestive physiology,³⁹ higher bile acid concentrations together with increased primary-to-secondary bile acid ratios were reproduced in the nutritive media of the M-ARILE. Since primary bile acids are essentially found in the bile used for M-ARILE media,⁷⁹ this study demonstrated efficient *in vitro* deconjugation of bile acids in the ileal compartment, likely driven by bacteria such as *Bacteroides* and *Clostridium*.^{80,81} Finally, nontargeted metabolomics provided new data on differential metabolites found in the human simulated ileum and colon environments. Metabolomes in the M-ARILE model consisted mostly of amino acids (alanine, glycine, isoleucine, lysine, proline, tyrosine, glutamic acid) and derivatives (pyroglutamic acid, norvaline), carbohydrates (galactose, inositol) and vitamins (nicotinic acid), in line with *in vivo* data in the healthy human ileum.⁷⁰ In contrast, in the colonic model, few nutrients are left, in accordance with human digestive physiology, where most food digestion processes and absorption take place in the small intestine.⁸²

Recent studies have shown that diet exerts a circadian influence on the richness, diversity and composition of the small intestine microbiota in humans, particularly within two hours postprandial.^{4,83} Therefore, as another novelty, we adapted the M-ARILE model to reproduce this diurnal variation in feeding status. RDA of the bacterial β -diversity revealed that the ileal microbiota was characterized by more dispersed profiles than the corresponding colon microbiota was, and this seemed to be mainly driven by the fed and fasted states. We also observed a bloom in the total bacterial load following a meal (data not

Table 4. Validation of the M-ARILE model through *in vitro-in vivo* comparisons regarding bacterial composition.

In vitro results in the M-ARILE were compared to *in vivo* data in the ileum of healthy human adults (based on *in vivo* analyses of aspirate or mucosal biopsies), regarding the most abundant phyla or families.

Phyla	Family	<i>In vivo</i>		<i>In vitro</i>		Validation	Reference
		Luminal	Mucosal	Luminal	Mucosal		
<i>Bacillota</i> (Firmicutes)	<i>Streptococcaceae</i>	+	+	/	/	✗	[47–50]
	<i>Staphylococcaceae</i>	+	+	/	/	✗	[47,48,50]
	<i>Veillonellaceae</i>	+	+	+	+	✓	[37,47,48,50,51]
	<i>Lachnospiraceae</i>	+	+	+	+	✓	[9,47,48,52]
	<i>Clostridiaceae</i>	+	+	+	+	✓	[9,47–50]
	<i>Peptococcaceae</i>	ND	+	/	/	✗	[50]
	<i>Peptostreptococcaceae</i>	+	+	+	+	✓	[47,50,53]
	<i>Ruminococcaceae</i>	ND	+	+	+	✓	[9,48,52]
	<i>Oscillospiraceae</i>	+	+	/	+	✓	[9,47]
	<i>Acidaminococcaceae</i>	+	ND	+	+	✓	[53]
	<i>Lactobacillaceae</i>	+	+	/	/	✗	[47,48,50,53]
	<i>Enterococcaceae</i>	+	+	+	+	✓	[37,50]
	<i>Bacillaceae</i>	ND	ND	+	/	/	ND
	<i>Erysipelotrichaceae</i>	ND	ND	+	/	/	ND
<i>Pseudomonadota</i> (Proteobacteria)	<i>Aeromonadaceae</i>	ND	+	/	/	✗	[9]
	<i>Enterobacteriaceae</i>	+	+	+	+	✓	[9,47,48,50,52,53]
	<i>Sutterellaceae</i>	+	ND	+	+	✓	[53]
	<i>Pasteurellaceae</i>	+	+	/	/	✗	[47,52]
	<i>Moraxellaceae</i>	ND	+	/	/	✗	[9,48]
	<i>Morganellaceae</i>	ND	+	/	/	✗	[50]
	<i>Haemophilus</i>	+	ND	/	/	✗	[47]
	<i>Burkholderiaceae</i>	ND	+	/	/	✗	[9]
	<i>Bacteroidaceae</i>	+	+	+	+	✓	[9,47,48,50,52,53]
	<i>Prevotellaceae</i>	+	+	+	/	✓	[9,47,48,53]
<i>Bacteroidota</i> (Bacteroidetes)	<i>Rikenellaceae</i>	+	+	+	+	✓	[48,53]
	<i>Tannerellaceae</i>	ND	+	+	+	✓	[52]
	<i>Barnesiellaceae</i>	+	ND	/	+	✓	[53]
	<i>Marinifilaceae</i>	ND	ND	+	/	/	ND
	<i>Bifidobacteriaceae</i>	+	+	+	+	✓	[9,47,48,52,53]
	<i>Actinomycetaceae</i>	+	+	/	/	✗	[47,48]
<i>Actinomycetota</i> (Actinobacteria)	<i>Micrococcaceae</i>	+	+	/	/	✗	[47,48]
	<i>Atopobiaceae</i>	+	ND	/	/	✗	[47]
	<i>Corynebacteriaceae</i>	ND	+	/	/	✗	[48,50]
	<i>Fusobacteriaceae</i>	+	+	/	/	✗	[9,49,50,52]
<i>Fusobacteriota</i>	<i>Verrucomicrobiaceae</i>	+	+	+	+	✓	[9,48,49]
<i>Verrucomicrobiota</i>	<i>Akkermansiaceae</i>	ND	+	/	+	✓	[51]
<i>Thermodesulfobacteriota</i>	<i>Desulfobivibrionaceae</i>	+	ND	+	+	✓	[53]
<i>Cyanobacteria</i>		+	+	/	/	✗	[9]
<i>Actinobacteriota</i>		ND	ND	+	+	/	ND
<i>Bdellovibrionota</i>		ND	ND	+	+	/	ND

+: found, /: not found in vitro, ND: no data in vivo; ✓: *in vitro* results are fully in accordance with *in vivo* data, ✓: *in vitro* and *in vivo* data showed some similarities, ✗: *in vitro* and *in vivo* data are not in accordance, /: no conclusion can be made due to lack of *in vivo* data.

shown), in line with a study in ileostomy patients where a significant increase in bacterial density was observed after the ingestion of a carbohydrate-rich meal.⁴⁴ Surprisingly, a lower α -diversity was observed during fed *versus* fasted state. These results cannot be challenged with *in vivo* data, but the decrease in α -diversity during the fed state might be linked to the fast growth of dominant microbes able to use available nutrients, ‘hiding’ low-abundance biomass.³⁷ In the M-ARILE, the fasted state was significantly associated with a bloom in *Akkermansiaceae* (and *Akkermansia* at the genus level). This finding is particularly interesting since human studies have shown that intermittent fasting during Ramadan was associated with positive changes in the gut microbiota community, including increased abundances of *Akkermansia*, *Bacteroides* and butyrate-producing *Lachnospiraceae*.⁸⁴ This circadian cycling of *Akkermansia*, which has never been reported in humans, would undeniably deserve further investigation in the future. This increase can be linked to the ability of *Akkermansia* to degrade mucin, supporting its survival in the fasted state and its survival advantage.^{30,85,86} Our *in vitro* study also provided interesting findings regarding the impact of feeding status on gut metabolites, with clearly distinct profiles regarding gas, SCFA, bile acids and metabolites identified by nontargeted metabolomics. Most of the changes in gas and SCFA production found in the M-ARILE corroborated the *in vivo* data, namely, lower SCFA production during the fasting state,⁷⁸ together with a decrease in CO₂ levels,⁴⁶ both reflecting a reduction in microbial activities. Additionally, higher butyrate and lower propionate levels were detected in ileostomy effluents

Table 5. Comparison of M-ARILE with currently published dynamic model of the human small intestine including microbiota.The *in vitro* model reproduces (✓), partially considers (✓) or does not simulate (✗) the corresponding parameter when simulating ileal conditions.

Name	Mono/multi compartmented	Digestive section simulated	Type of fermentation	Type of microbiota	Physicochemical parameters					Medium composition (g/L)										Digestive enzymes: Pancreatin	Fasted and fed conditions	Anaerobiosis	Mucos-associated microbiota	Eukaryota and/or Archaea monitoring	Validation in vitro vs in vivo	References
					pH control	Temperature control (°C)	Transit time (h)	Stirring	Intestinal absorption	Redox monitoring	Fibers	Simple carbohydrates	Proteins	Lipids	Oligosaccharides	Bile acids	Digestive enzymes: Pancreatin	Fasted and fed conditions	Anaerobiosis							
The smallest intestine (TSI)	Mono	Duodenum jejunum ileum	B	Consortium of 7 bacteria	✓	✓	2 h (D) 4 h (J) 2 h (I)	170 rpm	✓	✗	✗	✗	✗	✗	✗	✓ Bile (10 mM)	✓	✓	✓	Flushing by N ₂	✗	✗	✗	✗	✗	[13]
TNO ileum model (TIM-1)	Mono	Ileum	SC	Faecal sample or ileostomy	✓	✓	3.5 h	membrane compression 150 rpm	✓	✗	✓	✗	✓	✗	✓	✓ Bile (2.025 g/L)	✓	✗	✓	Flushing by N ₂	✗	✗	✗	✗	✗	[12]
M-SHIME	Multi	Stomach-duodenum-jejunum combined ileum, ascending colon ileum	SC	Faecal samples/Consortium of 12 bacteria	✓	✓	3 h (I) 20 h (AC)		✗	✗	✓	✓	✓	✗	✓	✓ Bile	✓	✓	✓	Flushing by N ₂	✓	✗	✗	✗	✗	[14,15]
M-ARILE	Mono	Ileum	C	Faecal samples	✓	✓	2 h	Day 300 rpm/ Night 100 rpm	✗	✓	✓	✓	✓	✓	✓	✓ Bile (4 mM fasted, 10 mM fed)	✓	✓	✓	Microbiota only	✓	✓	✓	✓	✓	The present study

AC: ascending colon; C: continuous; D: duodenum; I: ileum; J: jejunum; SC: semi-continuous; M-ARILE: Mucosal Artificial Ileum; M-SHIME: Mucosal Simulator of Human Intestinal Microbial Ecosystem; TSI: The Small Intestine.

during morning compared to afternoon sampling, findings that are consistent with fasted *versus* fed state results from the M-ARILE model.⁴⁴ Finally, amino acid contents were higher in the fed state, which is in line with the increase in protein intake supplied by the rich medium. Metabolite derivatives from amino acids (uracil, xanthine, ornithine) were also found in higher abundance in the fed state, corroborating the protein metabolism by the ileal microbiome described *in vivo*.⁴⁴

Our new model represents a significant step forward in the *in vitro* simulation of the human ileal microbiome under both fasted and fed states. Given that the small intestine is the primary site for nutrient and drug absorption in humans, M-ARILE holds valuable potential for many nutritional and pharmaceutical applications. Notably, the current model can serve as a versatile platform for studying the impact of the ileal microbiota on food digestibility and micronutrient bioaccessibility, as well as drug metabolism by ileal microbes, which may impact both its availability and efficacy.^{54,87} In addition, since some food-borne pathogens, such as *Escherichia coli* pathotypes, *Salmonella* and *Listeria*⁸⁸ constitute a primary colonization site in the human distal small intestine, the M-ARILE holds great potential for unravelling their complex relationships with ileal microbial communities, which may impact both pathogen colonization and virulence.^{89,90} This may foster the development of novel non-antibiotic therapeutic strategies, which are based on prebiotics, probiotics or vegetal extracts.⁹¹ Notably, by capturing interindividual variability in the gut microbiota, the ileal model will contribute to move toward personalized nutrition and medicine in the gut microbiome field. However, M-ARILE clearly lack key host components, such as intestinal cells, as well as neuroendocrine signaling and absorption mechanisms, which can shape the composition and functions of the gut microbiota. To better integrate host-microbiota interactions in the ileal compartment, future improvements should consider the coupling of the M-ARILE model with epithelial and/or immune cells. Lastly, it would be of great interest to adapt the M-ARILE not only to physiological but also to pathological conditions, where a dysbiosis in ileal microbiota has been described, such as inflammatory bowel diseases,⁹² small intestinal bacterial overgrowth⁹³ or obesity.⁹⁴

Ethics statement

All donors provided written, informed consent to participate in the study. The use of fecal microbiota of human origin was approved by the French Ethical Research Committee (Comité de protection des personnes Ouest VI) under registration number MEDIS MICROVITRO 2022-A02066–37.

Disclosure of potential conflicts of interest

The authors declare that they have no known of competing financial interests or personal relationships that could have appeared to influence the work reported in this paper.

Acknowledgments

This work was partially funded by the European Commission's Horizon 2020 Research and Innovation Program via the Innovative Training Network Marie Skłodowska-Curie COL_RES project under grant agreement No 956279. XD acknowledges the support from the la Caixa" Foundation (ID 100010434) via the Junior Leader Fellowship LCF/BQ/PR21/11840001 and from the Spanish State Research Agency (AEI/10.13039/501100011033) grant PID2024-159303OB-I00. We are grateful to the Mésocentre Clermont Auvergne University for providing computing and storage resources. Computations have been performed on the supercomputer facilities of the Mésocentre Clermont Auvergne University.

ORCID

Tom Van de Wiele  0000-0001-6854-5689

Data availability statement

Raw data are available at NCBI under the Sequence Read Archive database in the BioProject PRJNA1175656.

References

- 1 Delbaere K, Roegiers I, Bron A, Durif C, Van de Wiele T, Blanquet-Diot S, Marinelli L. The small intestine: dining table of host–microbiota meetings. *FEMS Microbiol Rev.* 2023;47:fuad022. doi: [10.1093/femsre/fuad022](https://doi.org/10.1093/femsre/fuad022).
- 2 Bernier J-J. Les aliments dans le tube digestif. Paris: Doin Editeurs; 1988.
- 3 Beaume J, Braconnier A, Dolley-Hitze T, Bertocchio J-P. Bicarbonate: de la physiologie aux applications thérapeutiques pour tout clinicien. *Nephrol Ther.* 2018;14:13–23. doi: [10.1016/j.nephro.2017.02.014](https://doi.org/10.1016/j.nephro.2017.02.014).
- 4 Yilmaz B, Fuhrer T, Morgenthaler D, Krupka N, Wang D, Spari D, Candinas D, Misselwitz B, Beldi G, Sauer U, et al. Plasticity of the adult human small intestinal stoma microbiota. *Cell Host Microbe.* 2022;30:1773–1787.e6. doi: [10.1016/j.chom.2022.10.002](https://doi.org/10.1016/j.chom.2022.10.002).
- 5 Johansson MEV, Ambort D, Pelaseyed T, Schütte A, Gustafsson JK, Ermund A, Subramani DB, Holmén-Larsson JM, Thomsson KA, Bergström JH, et al. Composition and functional role of the mucus layers in the intestine. *Cell Mol Life Sci.* 2011;68:3635–3641. doi: [10.1007/s00018-011-0822-3](https://doi.org/10.1007/s00018-011-0822-3).
- 6 Martinez-Guryn K, Leone V, Chang EB. Regional diversity of the gastrointestinal microbiome. *Cell Host Microbe.* 2019;26:314–324. doi: [10.1016/j.chom.2019.08.011](https://doi.org/10.1016/j.chom.2019.08.011).
- 7 Cummings JH, Pomare EW, Branch WJ, Naylor CP, Macfarlane GT. Short chain fatty acids in human large intestine, portal, hepatic and venous blood. *Gut.* 1987;28:1221–1227. doi: [10.1136/gut.28.10.1221](https://doi.org/10.1136/gut.28.10.1221).
- 8 Banaszak M, Górna I, Woźniak D, Przysławski J, Drzymała-Czyż S. Association between gut dysbiosis and the occurrence of SIBO, LIBO, SIFO and IMO. *Microorganisms.* 2023;11:573. doi: [10.3390/microorganisms11030573](https://doi.org/10.3390/microorganisms11030573).
- 9 Fan HN, Zhu P, Lu YM, Guo JH, Zhang J, Qu GQ, Zhu JS. Mild changes in the mucosal microbiome during terminal ileum inflammation. *Microb Pathog.* 2020;142:104104. doi: [10.1016/j.micpath.2020.104104](https://doi.org/10.1016/j.micpath.2020.104104).
- 10 Villmones HC, Haug ES, Ulvestad E, Grude N, Stenstad T, Halland A, Kommedal Ø. Species level description of the human ileal bacterial microbiota. *Sci Rep.* 2018;8:4736. doi: [10.1038/s41598-018-23198-5](https://doi.org/10.1038/s41598-018-23198-5).
- 11 Kastl AJ, Terry NA, Wu GD, Albenberg LG. The structure and function of the human small intestinal microbiota: current understanding and future directions. *Cell Mol Gastroenterol Hepatol.* 2020;9:33–45. doi: [10.1016/j.jcmgh.2019.07.006](https://doi.org/10.1016/j.jcmgh.2019.07.006).
- 12 Stolaki M, Minekus M, Venema K, Lahti L, Smid EJ, Kleerebezem M, Zoetendal EG. Microbial communities in a dynamic in vitro model for the human ileum resemble the human ileal microbiota. *FEMS Microbiol Ecol.* 2019;95:fiz096. doi: [10.1093/femsec/fiz096](https://doi.org/10.1093/femsec/fiz096).
- 13 Cieplak T, Wiese M, Nielsen S, Van de Wiele T, van den Berg F, Nielsen DS. The Smallest Intestine (TSI)—a low volume in vitro model of the small intestine with increased throughput. *FEMS Microbiol Lett.* 2018;365:fny231. doi: [10.1093/femsle/fny231](https://doi.org/10.1093/femsle/fny231).
- 14 Roussel C, De Paepe K, Galia W, De Bodt J, Chalancon S, Leriche F, Ballet N, Denis S, Alric M, Van de Wiele T, et al. Spatial and temporal modulation of enterotoxigenic *E. coli* H10407 pathogenesis and interplay with microbiota in human gut models. *BMC Biol.* 2020;18:141. doi: [10.1186/s12915-020-00860-x](https://doi.org/10.1186/s12915-020-00860-x).
- 15 Deyaert S, Moens F, Pirovano W, van den Bogert B, Klaessens ES, Marzorati M, Van de Wiele T, Kleerebezem M, Van den Abbeele P. Development of a reproducible small intestinal microbiota model and its integration into the SHIME®-system, a dynamic *in vitro* gut model. *Front Microbiol.* 2023;13 1054061. doi: [10.3389/fmicb.2022.1054061](https://doi.org/10.3389/fmicb.2022.1054061).
- 16 Deschamps C, Fournier E, Uriot O, Lajoie F, Verdier C, Comtet-Marre S, Thomas M, Kapel N, Cherbuy C, Alric M, et al. Comparative methods for fecal sample storage to preserve gut microbial structure and function in

- an in vitro model of the human colon. *Appl Microbiol Biotechnol.* **2020**;104:10233–10247. doi: [10.1007/s00253-020-10959-4](https://doi.org/10.1007/s00253-020-10959-4).
- 17 Etienne-Mesmin L, Meslier V, Uriot O, Fournier E, Deschamps C, Denis S, David A, Jegou S, Morabito C, Quinquis B, et al. In vitro modelling of oral microbial invasion in the human colon. *Microbiol Spectr.* **2023**;11:e0434422. doi: [10.1128/spectrum.04344-22](https://doi.org/10.1128/spectrum.04344-22).
 - 18 Fournier E, Denis S, Dominicis A, Van de Wiele T, Alric M, Mercier-Bonin M, Etienne-Mesmin L, Blanquet-Diot S. A child is not an adult: development of a new in vitro model of the toddler colon. *Appl Microbiol Biotechnol.* **2022**;106:7315–7336. doi: [10.1007/s00253-022-12199-0](https://doi.org/10.1007/s00253-022-12199-0).
 - 19 Yu Y, Lee C, Kim J, Hwang S. Group-specific primer and probe sets to detect methanogenic communities using quantitative real-time polymerase chain reaction. *Biotechnol Bioeng.* **2005**;89:670–679. doi: [10.1002/bit.20347](https://doi.org/10.1002/bit.20347).
 - 20 Bacchetti De Gregoris T, Aldred N, Clare AS, Burgess JG. Improvement of phylum- and class-specific primers for real-time PCR quantification of bacterial taxa. *J Microbiol Methods.* **2011**;86:351–356. doi: [10.1016/j.mimet.2011.06.010](https://doi.org/10.1016/j.mimet.2011.06.010).
 - 21 Klindworth A, Pruesse E, Schweer T, Peplies J, Quast C, Horn M, Glöckner FO. Evaluation of general 16S ribosomal RNA gene PCR primers for classical and next-generation sequencing-based diversity studies. *Nucleic Acids Res.* **2013**;41:e1–e1. doi: [10.1093/nar/gks808](https://doi.org/10.1093/nar/gks808).
 - 22 Takai K, Horikoshi K. Rapid detection and quantification of members of the archaeal community by quantitative PCR using fluorogenic probes. *Appl Environ Microbiol.* **2000**;66:5066–5072. doi: [10.1128/AEM.66.11.5066-5072.2000](https://doi.org/10.1128/AEM.66.11.5066-5072.2000).
 - 23 Theil S, Rifa E. rANOMALY: Amplicon workflow for Microbial community Analysis. *F1000Res.* **2021**;10:7. doi: [10.12688/f1000research.27268.1](https://doi.org/10.12688/f1000research.27268.1).
 - 24 Callahan BJ, McMurdie PJ, Rosen MJ, Han AW, Johnson AJA, Holmes SP. DADA2: high-resolution sample inference from Illumina amplicon data. *Nat Methods.* **2016**;13:581–583. doi: [10.1038/nmeth.3869](https://doi.org/10.1038/nmeth.3869).
 - 25 Murali A, Bhargava A, Wright ES. IDTAXA: a novel approach for accurate taxonomic classification of microbiome sequences. *Microbiome.* **2018**;6:140. doi: [10.1186/s40168-018-0521-5](https://doi.org/10.1186/s40168-018-0521-5).
 - 26 Quast C, Pruesse E, Yilmaz P, Gerken J, Schweer T, Yarza P, Peplies J, Glöckner FO. The SILVA ribosomal RNA gene database project: improved data processing and web-based tools. *Nucleic Acids Res.* **2013**;41:D590–D596. doi: [10.1093/nar/gks1219](https://doi.org/10.1093/nar/gks1219).
 - 27 Schliep KP. Phangorn: phylogenetic analysis in R. *Bioinformatics.* **2011**;27:592–593. doi: [10.1093/bioinformatics/btq706](https://doi.org/10.1093/bioinformatics/btq706).
 - 28 de Cripian SM, Arora T, Olomí A, Finch JP, Domingo-Almenara X. Untargeted GC-MS Data Processing and Metabolite Identification Using eRah. In J Ivanisevic, M Giera (Eds.), *A Practical Guide to Metabolomics Applications in Health and Disease: From Samples to Insights into Metabolism.* **2023.** pp. 125–157 Cham: Springer International Publishing. doi:10.1007/978-3-031-44256-8_6.
 - 29 Domingo-Almenara X, Brezmes J, Vinaixa M, Samino S, Ramirez N, Ramon-Krauel M, Lerin C, Díaz M, Ibáñez L, Correig X, et al. eRah: a computational tool integrating spectral deconvolution and alignment with quantification and identification of metabolites in GC/MS-based metabolomics. *Anal Chem.* **2016**;88:9821–9829. doi: [10.1021/acs.analchem.6b02927](https://doi.org/10.1021/acs.analchem.6b02927).
 - 30 Liu C, Cui Y, Li X, Yao M. microeco: an R package for data mining in microbial community ecology. *FEMS Microbiol Ecol.* **2021**;97:fiaa255. doi: [10.1093/femsec/fiaa255](https://doi.org/10.1093/femsec/fiaa255).
 - 31 Borgström B, Dahlqvist A, Lundh G, Sjövall J. Studies of intestinal digestion and absorption in the human1. *J Clin Invest.* **1957**;36:1521–1536. doi: [10.1172/JCI103549](https://doi.org/10.1172/JCI103549).
 - 32 Evans DF, Pye G, Bramley R, Clark AG, Dyson TJ, Hardcastle JD. Measurement of gastrointestinal pH profiles in normal ambulant human subjects. *Gut.* **1988**;29:1035–1041. doi: [10.1136/gut.29.8.1035](https://doi.org/10.1136/gut.29.8.1035).
 - 33 Fallingborg J, Pedersen P, Jacobsen BA. Small intestinal transit time and intraluminal pH in ileocecal resected patients with crohn's disease. *Dig Dis Sci.* **1998**;43:702–705. doi: [10.1023/A:1018893409596](https://doi.org/10.1023/A:1018893409596).
 - 34 Alqahtani MS, Kazi M, Alsenaidy MA, Ahmad MZ. Advances in oral drug delivery. *Front Pharmacol.* **2021**;12:618411. doi: [10.3389/fphar.2021.618411](https://doi.org/10.3389/fphar.2021.618411).
 - 35 Koziol M, Grimm M, Becker D, Iordanov V, Zou H, Shimizu J, Wanke C, Garbacz G, Weitschies W. Investigation of pH and temperature profiles in the GI tract of fasted human subjects using the intellicap® system. *J Pharm Sci.* **2015**;104:2855–2863. doi: [10.1002/jps.24274](https://doi.org/10.1002/jps.24274).
 - 36 Shkempi B, Huppertz T. Calcium absorption from food products: food matrix effects. *Nutrients.* **2021**;14:180. doi: [10.3390/nu14010180](https://doi.org/10.3390/nu14010180).
 - 37 Booiijink CCGM, El-Aidy S, Rajilić-Stojanović M, Heilig HGHJ, Troost FJ, Smidt H, Kleerebezem M, De Vos WM, Zoetendal EG. High temporal and inter-individual variation detected in the human ileal microbiota. *Environ Microbiol.* **2010**;12:3213–3227. doi: [10.1111/j.1462-2920.2010.02294.x](https://doi.org/10.1111/j.1462-2920.2010.02294.x).
 - 38 Dahlgren D, Venczel M, Ridoux J-P, Skjöld C, Müllertz A, Holm R, Augustijns P, Hellström P, Lennernäs H. Fasted and fed state human duodenal fluids: characterization, drug solubility, and comparison to simulated fluids and with human bioavailability. *Eur J Pharm Biopharm.* **2021**;163:240–251. doi: [10.1016/j.ejpb.2021.04.005](https://doi.org/10.1016/j.ejpb.2021.04.005).
 - 39 Ciaula AD, Garruti G, Baccetto RL, Molina-Molina E, Bonfrate L, Portincasa P, Di Ciaula A, Lunardi Baccetto R, Wang DQ. Bile acid physiology. *Ann Hepatol.* **2017**;16:4–14. doi: [10.5604/01.3001.0010.5493](https://doi.org/10.5604/01.3001.0010.5493).
 - 40 Northfield TC, McColl I. Postprandial concentrations of free and conjugated bile acids down the length of the normal human small intestine. *Gut.* **1973**;14:513–518. doi: [10.1136/gut.14.7.513](https://doi.org/10.1136/gut.14.7.513).

- 41 Riethorst D, Mols R, Duchateau G, Tack J, Brouwers J, Augustijns P. Characterization of human duodenal fluids in fasted and fed state conditions. *J Pharm Sci.* 2016;105:673–681. doi: [10.1002/jps.24603](https://doi.org/10.1002/jps.24603).
- 42 de Aguiar Vallim TQ, Tarling EJ, Edwards PA. Pleiotropic roles of bile acids in metabolism. *Cell Metabolism.* 2013;17:657–669. doi: [10.1016/j.cmet.2013.03.013](https://doi.org/10.1016/j.cmet.2013.03.013).
- 43 Duboc H, Coffin B, Siproudhis L. Disruption of circadian rhythms and gut motility: An overview of underlying mechanisms and associated pathologies. *J Clin Gastroenterol.* 2020;54:405–414. doi: [10.1097/MCG.0000000000001333](https://doi.org/10.1097/MCG.0000000000001333).
- 44 Zoetendal EG, Raes J, van den Bogert B, Arumugam M, Booijink CC, Troost FJ, Bork P, Wels M, de Vos WM, Kleerebezem M. The human small intestinal microbiota is driven by rapid uptake and conversion of simple carbohydrates. *ISME J.* 2012;6:1415–1426. doi: [10.1038/ismej.2011.212](https://doi.org/10.1038/ismej.2011.212).
- 45 Berean KJ, Ha N, Ou JZ, Chrimes AF, Grando D, Yao CK, Muir JG, Ward SA, Burgell RE, Gibson PR, et al. The safety and sensitivity of a telemetric capsule to monitor gastrointestinal hydrogen production in vivo in healthy subjects: a pilot trial comparison to concurrent breath analysis. *Aliment Pharmacol Ther.* 2018;48:646–654. doi: [10.1111/apt.14923](https://doi.org/10.1111/apt.14923).
- 46 Kalantar-Zadeh K, Berean KJ, Burgell RE, Muir JG, Gibson PR. Intestinal gases: influence on gut disorders and the role of dietary manipulations. *Nat Rev Gastroenterol Hepatol.* 2019;16:733–747. doi: [10.1038/s41575-019-0193-z](https://doi.org/10.1038/s41575-019-0193-z).
- 47 van Trijp MPH, Rios-Morales M, Witteman B, Abegaz F, Gerding A, An R, Koehorst M, Evers B, van Dongen KC, Zoetendal EG, et al. Intraintestinal fermentation of fructo- and galacto-oligosaccharides and the fate of short-chain fatty acids in humans. *iScience.* 2024;27:109208. doi: [10.1016/j.isci.2024.109208](https://doi.org/10.1016/j.isci.2024.109208).
- 48 Vuik F, Dicksved J, Lam S, Fuhler G, van der Laan L, van de Winkel A, Konstantinov S, Spaander M, Peppelenbosch M, Engstrand L, et al. Composition of the mucosa-associated microbiota along the entire gastrointestinal tract of human individuals. *United Eur Gastroenterol J.* 2019;7:897–907. doi: [10.1177/2050640619852255](https://doi.org/10.1177/2050640619852255).
- 49 Wang M, Ahrné S, Jeppsson B, Molin G. Comparison of bacterial diversity along the human intestinal tract by direct cloning and sequencing of 16S rRNA genes. *FEMS Microbiol Ecol.* 2005;54:219–231. doi: [10.1016/j.femsec.2005.03.012](https://doi.org/10.1016/j.femsec.2005.03.012).
- 50 Zilberstein B, Quintanilha AG, Santos MAA, Pajecski D, Moura EG, Alves PRA, Filho FM, Souza JAUD, Gama-Rodrigues J. Digestive tract microbiota in healthy volunteers. *Clinics.* 2007;62:47–56. doi: [10.1590/S1807-59322007000100008](https://doi.org/10.1590/S1807-59322007000100008).
- 51 Nagasue T, Hirano A, Torisu T, Umeno J, Shibata H, Moriyama T, Kawasaki K, Fujioka S, Fuyuno Y, Matsuno Y, et al. The compositional structure of the small intestinal microbial community via balloon-assisted enteroscopy. *Digestion.* 2022;103:308–318. doi: [10.1159/000524023](https://doi.org/10.1159/000524023).
- 52 Kashiwagi S, Naito Y, Inoue R, Takagi T, Nakano T, Inada Y, Fukui A, Katada K, Mizushima K, Kamada K, et al. Mucosa-associated microbiota in the gastrointestinal tract of healthy Japanese subjects. *Digestion.* 2020;101:107–120. doi: [10.1159/000496102](https://doi.org/10.1159/000496102).
- 53 Shalon D, Culver RN, Grembi JA, Folz J, Treit PV, Shi H, Rosenberger FA, Dethlefsen L, Meng X, Yaffe E, et al. Profiling the human intestinal environment under physiological conditions. *Nature.* 2023;617:581–591. doi: [10.1038/s41586-023-05989-7](https://doi.org/10.1038/s41586-023-05989-7).
- 54 Ruigrok RAAA, Weersma RK, Vich Vila A. The emerging role of the small intestinal microbiota in human health and disease. *Gut Microbes.* 2023;15:2201155. doi: [10.1080/19490976.2023.2201155](https://doi.org/10.1080/19490976.2023.2201155).
- 55 EN - EUR-Lex. n.d. Directive - 2010/63.
- 56 Yersin S, Vonaesch P. Small intestinal microbiota: from taxonomic composition to metabolism. *Trends Microbiol.* 2024;32:970–983. doi: [10.1016/j.tim.2024.02.013](https://doi.org/10.1016/j.tim.2024.02.013).
- 57 Ringel Y, Maharshak N, Ringel-Kulka T, Wolber EA, Sartor RB, Carroll IM. High throughput sequencing reveals distinct microbial populations within the mucosal and luminal niches in healthy individuals. *Gut Microbes.* 2015;6:173–181. doi: [10.1080/19490976.2015.1044711](https://doi.org/10.1080/19490976.2015.1044711).
- 58 Wu M, Li P, Li J, An Y, Wang M, Zhong G. The differences between luminal microbiota and mucosal microbiota in mice. *J Microbiol Biotechnol.* 2020;30:287–295. doi: [10.4014/jmb.1908.08037](https://doi.org/10.4014/jmb.1908.08037).
- 59 Deschamps C, Denis S, Humbert D, Priymenko N, Chalancon S, De Bodt J, Van de Wiele T, Ipharraguerre I, Alvarez-Acero I, Achard C, et al. Canine mucosal artificial colon: development of a new colonic *in vitro* model adapted to dog sizes. *Appl Microbiol Biotechnol.* 2024;108:166. doi: [10.1007/s00253-023-12987-2](https://doi.org/10.1007/s00253-023-12987-2).
- 60 Gresse R, Chaucheyras-Durand F, Denis S, Beaumont M, Van de Wiele T, Forano E, Blanquet-Diot S. Weaning-associated feed deprivation stress causes microbiota disruptions in a novel mucin-containing *in vitro* model of the piglet colon (MPigut-IVM). *J Animal Sci Biotechnol.* 2021;12:75. doi: [10.1186/s40104-021-00584-0](https://doi.org/10.1186/s40104-021-00584-0).
- 61 Van den Abbeele P, Grootaert C, Possemiers S, Verstraete W, Verbeken K, Van de Wiele T. *In vitro* model to study the modulation of the mucin-adhered bacterial community. *Appl Microbiol Biotechnol.* 2009;83:349–359. doi: [10.1007/s00253-009-1947-2](https://doi.org/10.1007/s00253-009-1947-2).
- 62 Paone P, Cani PD. Mucus barrier, mucins and gut microbiota: the expected slimy partners?. *Gut.* 2020;69:2232–2243. doi: [10.1136/gutjnl-2020-322260](https://doi.org/10.1136/gutjnl-2020-322260).
- 63 Navarro-Garcia F. Serine proteases autotransporter of Enterobacteriaceae: structures, subdomains, motifs, functions, and targets. *Mol Microbiol.* 2023;120:178–193. doi: [10.1111/mmi.15116](https://doi.org/10.1111/mmi.15116).
- 64 Herrero ER, Fernandes S, Verspecht T, Ugarte-Berzal E, Boon N, Proost P, Bernaerts K, Quirynen M, Teughels W. Dysbiotic biofilms deregulate the periodontal inflammatory response. *J Dent Res.* 2018;97:547–555. doi: [10.1177/0022034517752675](https://doi.org/10.1177/0022034517752675).

- 65 Louis P, Flint HJ. Formation of propionate and butyrate by the human colonic microbiota. *Environ Microbiol*. 2017;19:29–41. doi: [10.1111/1462-2920.13589](https://doi.org/10.1111/1462-2920.13589).
- 66 Fournier E, Leveque M, Ruiz P, Ratel J, Durif C, Chalancon S, Amiard F, Edely M, Bezirard V, Gaultier E, et al. Microplastics: what happens in the human digestive tract? first evidences in adults using in vitro gut models. *J Hazard Mater*. 2023;442:130010. doi: [10.1016/j.jhazmat.2022.130010](https://doi.org/10.1016/j.jhazmat.2022.130010).
- 67 McCallum G, Tropini C. The gut microbiota and its biogeography. *Nat Rev Microbiol*. 2024;22:105–118. doi: [10.1038/s41579-023-00969-0](https://doi.org/10.1038/s41579-023-00969-0).
- 68 Etienne-Mesmin L, Chassaing B, Desvaux M, De Paepe K, Gresse R, Sauvaitre T, Forano E, de Wiele TV, Schüller S, Juge N, et al. Experimental models to study intestinal microbes-mucus interactions in health and disease. *FEMS Microbiol Rev*. 2019;43:457–489. doi: [10.1093/femsre/fuz013](https://doi.org/10.1093/femsre/fuz013).
- 69 Patrascu O, Béguet-Crespel F, Marinelli L, Le Chatelier E, Abraham A-L, Leclerc M, Klopp C, Terrapon N, Henrissat B, Blottière HM, et al. A fibrolytic potential in the human ileum mucosal microbiota revealed by functional metagenomic. *Sci Rep*. 2017;7:40248. doi: [10.1038/srep40248](https://doi.org/10.1038/srep40248).
- 70 Folz J, Culver RN, Morales JM, Grembi J, Triadafilopoulos G, Relman DA, Huang KC, Shalon D, Fiehn O. Human metabolome variation along the upper intestinal tract. *Nat Metab*. 2023;5:777–788. doi: [10.1038/s42255-023-00777-z](https://doi.org/10.1038/s42255-023-00777-z).
- 71 Kalantar-Zadeh K, Berean KJ, Ha N, Chrimes AF, Xu K, Grando D, Ou JZ, Pillai N, Campbell JL, Brkljača R, et al. A human pilot trial of ingestible electronic capsules capable of sensing different gases in the gut. *Nat Electron*. 2018;1:79–87. doi: [10.1038/s41928-017-0004-x](https://doi.org/10.1038/s41928-017-0004-x).
- 72 Espey MG. Role of oxygen gradients in shaping redox relationships between the human intestine and its microbiota. *Free Radic Biol Med*. 2013;55:130–140. doi: [10.1016/j.freeradbiomed.2012.10.554](https://doi.org/10.1016/j.freeradbiomed.2012.10.554).
- 73 Pochart P, Lémann F, Flourie B, Pellier P, Goderel I, Rambaud J-C. Pyxigraphic sampling to enumerate methanogens and anaerobes in the right colon of healthy humans. *Gastroenterology*. 1993;105(5):1281–1285. doi: [10.1016/0016-5085\(93\)90129-Z](https://doi.org/10.1016/0016-5085(93)90129-Z).
- 74 Gaci N, Borrel G, Tottey W, O'Toole PW, Brugère J-F. Archaea and the human gut: new beginning of an old story. *World J Gastroenterol*. 2014;20:16062. doi: [10.3748/wjg.v20.i43.16062](https://doi.org/10.3748/wjg.v20.i43.16062).
- 75 Hoegenauer C, Hammer HF, Mahnert A, Moissl-Eichinger C. Methanogenic archaea in the human gastro-intestinal tract. *Nat Rev Gastroenterol Hepatol*. 2022;19:805–813. doi: [10.1038/s41575-022-00673-z](https://doi.org/10.1038/s41575-022-00673-z).
- 76 Florin TH, Woods HJ. Inhibition of methanogenesis by human bile. *Gut*. 1995;37:418–421. doi: [10.1136/gut.37.3.418](https://doi.org/10.1136/gut.37.3.418).
- 77 Koskinen K, Pausan MR, Perras AK, Beck M, Bang C, Mora M, Schilhabel A, Schmitz R, Moissl-Eichinger C, Schleper CM, et al. First insights into the diverse human archaeome: specific detection of archaea in the gastro-intestinal tract, lung, and nose and on skin. *mBio*. 2017;8:10.1128/mbio.00824-17. doi: [10.1128/mbio.00824-17](https://doi.org/10.1128/mbio.00824-17).
- 78 Caffaratti C, Plazy C, Mery G, Tidjani A-R, Fiorini F, Thiroux S, Toussaint B, Hannani D, Le Gouvellec A. What we know so far about the metabolite-mediated microbiota-intestinal immunity dialogue and how to hear the sound of this crosstalk. *Metabolites*. 2021;11:406. doi: [10.3390/metabo11060406](https://doi.org/10.3390/metabo11060406).
- 79 Larabi AB, Masson HLP, Bäumler AJ. Bile acids as modulators of gut microbiota composition and function. *Gut Microbes*. 2023;15:2172671. doi: [10.1080/19490976.2023.2172671](https://doi.org/10.1080/19490976.2023.2172671).
- 80 Jones BV, Begley M, Hill C, Gahan CGM, Marchesi JR. Functional and comparative metagenomic analysis of bile salt hydrolase activity in the human gut microbiome. *Proc Natl Acad Sci U S A*. 2008;105:13580–13585. doi: [10.1073/pnas.0804437105](https://doi.org/10.1073/pnas.0804437105).
- 81 Rowland I, Gibson G, Heinken A, Scott K, Swann J, Thiele I, Tuohy K. Gut microbiota functions: metabolism of nutrients and other food components. *Eur J Nutr*. 2018;57:1–24. doi: [10.1007/s00394-017-1445-8](https://doi.org/10.1007/s00394-017-1445-8).
- 82 Jensen BAH, Heyndrickx M, Jonkers D, Mackie A, Millet S, Naghibi M, Pærregaard SI, Pot B, Saulnier D, Sina C, et al. Small intestine vs. colon ecology and physiology: why it matters in probiotic administration. *CR Med*. 2023;4:101190. doi: [10.1016/j.xcrm.2023.101190](https://doi.org/10.1016/j.xcrm.2023.101190).
- 83 Zheng D, Ratiner K, Elinav E. Circadian Influences of Diet on the Microbiome and Immunity. *Trends Immunol*. 2020;41:512–530. doi: [10.1016/j.it.2020.04.005](https://doi.org/10.1016/j.it.2020.04.005).
- 84 Angoorani P, Ejtahed H-S, Hasani-Ranjbar S, Siadat SD, Soroush AR, Larijani B. Gut microbiota modulation as a possible mediating mechanism for fasting-induced alleviation of metabolic complications: a systematic review. *Nutr Metab (Lond)*. 2021;18:105. doi: [10.1186/s12986-021-00635-3](https://doi.org/10.1186/s12986-021-00635-3).
- 85 Derrien M, Vaughan EE, Plugge CM, de Vos WM. *Akkermansia muciniphila* gen. nov., sp. nov., a human intestinal mucin-degrading bacterium. *Int J Syst Evol Microbiol*. 2004;54:1469–1476. doi: [10.1099/ijs.0.02873-0](https://doi.org/10.1099/ijs.0.02873-0).
- 86 Liu MJ, Yang JY, Yan ZH, Hu S, Li JQ, Xu ZX, Jian YP. Recent findings in *Akkermansia muciniphila*-regulated metabolism and its role in intestinal diseases. *Clin Nutr*. 2022;41(10):2333–2344. doi: [10.1016/j.clnu.2022.08.029](https://doi.org/10.1016/j.clnu.2022.08.029).
- 87 Doré J, Multon M-C, Béhier J-M, Affagard H, Andremont A, Barthélémy P, Batista R, Bonneville M, Bonny C, Boyaval G, et al. Microbiote intestinale: qu'en attendre au plan physiologique et thérapeutique? *Thérapies*. 2017;72:1–19. doi: [10.1016/j.therap.2017.01.001](https://doi.org/10.1016/j.therap.2017.01.001).
- 88 Foster-Nyarko E, Pallen MJ. The microbial ecology of *Escherichia coli* in the vertebrate gut. *FEMS Microbiol Rev*. 2022;46:fuac008. doi: [10.1093/femsre/fuac008](https://doi.org/10.1093/femsre/fuac008).
- 89 Akritidou T, Akkermans S, Smet C, Gaspari S, Sharma C, Matthews E, Van Impe JF. Gut microbiota of the small intestine as an antimicrobial barrier against foodborne pathogens: impact of diet on the survival of *S.*

- Typhimurium and *L. monocytogenes* during in vitro digestion. *Food Res Int.* **2023**;173:113292. doi: [10.1016/j.foodres.2023.113292](https://doi.org/10.1016/j.foodres.2023.113292).
- 90 Zhang C, Derrien M, Levenez F, Brazeilles R, Ballal SA, Kim J, Degivry M, Quéré G, Garault P, van Hylckama Vlieg JET, et al. Ecological robustness of the gut microbiota in response to ingestion of transient food-borne microbes. *The ISME Journal.* **2016**;10:2235–2245. doi: [10.1038/ismej.2016.13](https://doi.org/10.1038/ismej.2016.13).
- 91 Sauvaitre T, Durif C, Sivignon A, Chalancon S, Van de Wiele T, Etienne-Mesmin L, Blanquet-Diot S. In vitro evaluation of dietary fiber anti-infectious properties against food-borne enterotoxigenic *Escherichia coli*. *Nutrients.* **2021**;13:3188. doi: [10.3390/nu13093188](https://doi.org/10.3390/nu13093188).
- 92 Hernández-Rocha C, Turpin W, Borowski K, Stempak JM, Sabic K, Gettler K, Tastad C, Chasteau C, Korie U, Hanna M, et al. After surgically induced remission, ileal and colonic mucosa-associated microbiota predicts Crohn's disease recurrence. *Clin Gastroenterol Hepatol.* **2024**. S1542356524005925. doi: [10.1016/j.cgh.2024.06.022](https://doi.org/10.1016/j.cgh.2024.06.022).
- 93 Li J, Zhang R, Ma J, Tang S, Li Yuan, Li Yi, Wan J. Mucosa-associated microbial profile is altered in small intestinal bacterial overgrowth. *Front Microbiol.* **2021**;12:710940. doi: [10.3389/fmicb.2021.710940](https://doi.org/10.3389/fmicb.2021.710940).
- 94 Steinbach E, Masi D, Ribeiro A, Serradas P, Le Roy T, Clément K. Upper small intestine microbiome in obesity and related metabolic disorders: a new field of investigation. *Metabolism.* **2024**;150:155712. doi: [10.1016/j.metabol.2023.155712](https://doi.org/10.1016/j.metabol.2023.155712).
- 95 Lotti C, Rubert J, Fava F, Tuohy K, Mattivi F, Vrhovsek U. Development of a fast and cost-effective gas chromatography–mass spectrometry method for the quantification of short-chain and medium-chain fatty acids in human biofluids. *Anal Bioanal Chem.* **2017**;409:5555–5567. doi: [10.1007/s00216-017-0493-5](https://doi.org/10.1007/s00216-017-0493-5).